

Invited paper presented at the “Thorium Energy Alliance 5th Annual Future of Energy Conference,” Loyola University, Regents Hall, Water Tower Campus, 111 Pearson, Chicago, IL 60611, Illinois ,USA, May 30 –31, 2013.

Fail-Safe, Source-Driven Thorium Reactors

Monish Singh and Magdi Ragheb

Department of Nuclear, Plasma and Radiological Engineering
University of Illinois at Urbana-Champaign,
216 Talbot Laboratory,
104 South Wright Street,
Urbana, Illinois 61801, USA.

<http://www.mragheb.com>

mragheb@illinois.edu

msingh22@illinois.edu

ABSTRACT

A source-driven nuclear reactor configuration with a unity infinite medium multiplication factor fission core is investigated for both fission and fusion-fission hybrid systems. Such configuration is thought to offer a desirable fail-safe reactor alternative in that the loss of the fission or the fusion neutron sources would automatically lead to a shut-down of the system into a stable subcritical state with an effective multiplication factor of less than unity. This is so since the fission core cannot maintain criticality without the presence of the neutron source.

A circulating liquid molten salt using the Th-U²³³ fuel cycle, where the fission products are continuously extracted, further contributes to the fail-safe characteristic by avoiding the cooling needed for the decay heat or afterheat after reactor shut-down. Through the extraction of the Pa²³³ relatively long-lived precursor isotope, and allowing it sufficient time to decay into its U²³³ daughter, breeding in either thermal or fast neutron spectra is a distinct possibility. The presence of trace amounts of U²³² and the strong gamma-emitting Tl²⁰⁸ daughter isotope offers a desirable non-proliferation characteristic for the cycle.

As a proof of principle, a simplified analytical one-group neutronics analysis is first attempted for the pure fission core system. An energy and material flows analysis conducted to estimate the support ratios in a coupled fusion-fission hybrid system, where the bred U²³³ fissile fuel is fed from a fusion-fission fuel factory to pure fission satellites, suggests that sufficient support ratios can be obtained if a conversion ratio that is close to unity can be obtained for the fission island in the coupled system.

This is then supplemented with numerical one-group criticality calculations using an iterative finite-difference methodology. Further, a more detailed multi-group Monte Carlo neutronics analysis of the fission core reactor driven by a U²³³ fission neutron source, Deuterium-Tritium (DT) and Deuterium-Deuterium (DD) fusion neutron sources was conducted using the MCNP5 computer code.

THE INFINITE MEDIUM MULTIPLICATION FACTOR

In an infinite medium, the flux assumes a constant value, no gradient exists, and hence there is no neutron leakage and we can define an infinite medium multiplication factor as:

$$k_{\infty} = \frac{\text{neutrons produced in current fission generation}}{\text{neutrons absorbed in previous fission generation}}$$

The infinite medium multiplication factor can be expressed in terms of the four-factor formula:

$$k_{\infty} = \eta \epsilon p f$$

where: η is the regeneration factor,
 ϵ is the fast fission factor,
 p is the resonance escape probability,
 f is the fuel utilization factor.

THE CRITICALITY EQUATION

We can define an effective multiplication factor as:

$$k_{eff} = k_{\infty f} \frac{1}{1 + L^2 B^2} = k_{\infty f th}$$

where: ℓ_{th} is the thermal neutrons non-leakage probability,

$$\ell_{th} = \frac{1}{1 + L^2 B^2}$$

where: ℓ_f is the fast neutrons non-leakage probability

$k_{eff} < 1$, for a subcritical reactor,

$k_{eff} > 1$, for a supercritical reactor,

$k_{eff} = 1$, for a just critical reactor.

Geometric buckling: $B_g^2 = \left(\frac{\pi}{R_{ex}}\right)^2 = B^2$,

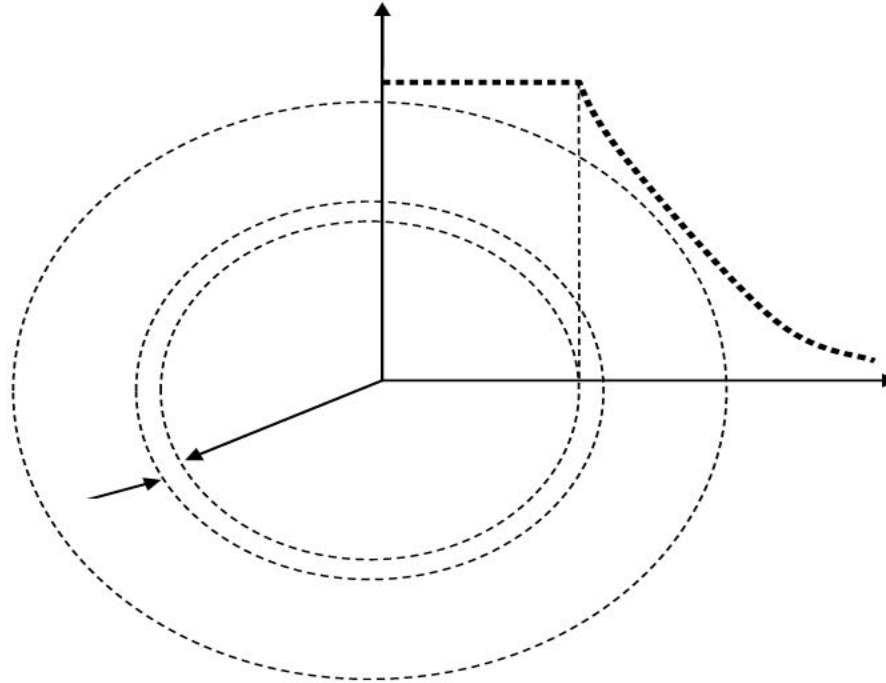
R_{ex} = extrapolated reactor radius for a sphere

I. EXACT ANALYTICAL SOLUTION

FAIL-SAFE REACTOR CORE

Consider a spherical or cylindrical reactor core with core radius R surrounded with an infinite reflector. If the core infinite medium multiplication factor is chosen to be exactly unity:

$$k_{\infty} = 1,$$



Geometry of a spherical core with an infinite reflector and a neutron source reflector interface.

The system would be essentially subcritical even with the presence of the reflector because of the leakage from the core to the reflector leading to a value of the effective multiplication factor of less than unity:

$$k_{eff} < 1$$

Assuming a thin thickness T of fissile material with a macroscopic absorption cross section Σ_a , and macroscopic fission cross section Σ_f , the neutron source introduces a net current at the interface equal to:

$$\begin{aligned}
 J_{\substack{\text{neutron} \\ \text{source}}} &= \nu \Sigma_f \phi_c(R) \cdot T - \Sigma_{aF} \phi_c(R) \cdot T \\
 &= \nu \frac{\Sigma_f}{\Sigma_{aF}} \Sigma_{aF} \phi_c(R) \cdot T - \Sigma_{aF} \phi_c(R) \cdot T \\
 &= (\eta_{\substack{\text{neutron} \\ \text{source}}} - 1) \Sigma_{aF} \phi_c(R) \cdot T
 \end{aligned}$$

where: $\phi_c(R)$ is the value of the flux at the core and reflector interface where the neutron source is introduced.

We can write diffusion equations for the core and reflector regions as:

$$\begin{aligned}
 \text{Core:} \quad & D_c \nabla^2 \phi_c - \Sigma_{ac} \phi_c + \eta_c \Sigma_{aFc} \phi_c = 0 \\
 \text{Reflector:} \quad & D_r \nabla^2 \phi_r - \Sigma_{ar} \phi_r = 0
 \end{aligned}$$

Now we can suggest that for a fast unmoderated reactor material in the core with unity resonance escape probability p and fast fission factor ϵ :

$$k_{\infty} = \eta_c \epsilon p f \quad \eta_c \cdot 1.1 \cdot f = \eta_c f$$

and:

$$\eta_c \sum_{aF} = \eta_c \frac{\sum_{aF}}{\sum_{ac}} \sum_{ac} = \eta_c f \sum_{ac} = k_{\infty} \sum_{ac}$$

Substituting in the core and reflector diffusion theory equations:

$$\nabla^2 \phi_c + \frac{(k_{\infty} - 1)}{L_c^2} \phi_c = 0, \quad L_c^2 = \frac{D_c}{\sum_{ac}}$$

$$\nabla^2 \phi_r - \frac{1}{L_r^2} \phi_r = 0, \quad L_r^2 = \frac{D_r}{\sum_{ar}}$$

If the material of the core is chosen with an infinite medium multiplication factor of unity, the material buckling in the core is:

$$B_c^2 = \frac{k_\infty - 1}{L_c^2} = \frac{1 - 1}{L_c^2} = 0$$

The zero buckling of the core means that a flat flux distribution exists in the core implying a uniform power distribution, a desirable feature leading to a uniform fuel burnup. In spherical geometry:

$$\begin{aligned}\nabla^2 \phi_c(r) &= 0, \\ \frac{1}{r^2} \frac{d}{dr} \left(r^2 \frac{d\phi_c(r)}{dr} \right) &= 0, \\ d \left(r^2 \frac{d\phi_c(r)}{dr} \right) &= C, \\ \frac{d\phi_c(r)}{dr} &= \frac{C}{r^2}, \forall r \neq 0, \\ d\phi_c(r) &= \int \frac{C}{r^2} dr \\ \phi_c(r) &= -\frac{C}{r} + F\end{aligned}$$

For a finite flux in the core, $C = 0$, and:

$$\phi_c(r) = F = \text{constant.}$$

The flux solution in the infinite reflector is:

$$\phi_r(r) = A \frac{e^{-\frac{r}{L_r}}}{r} + G \frac{e^{+\frac{r}{L_r}}}{r}$$

For a finite flux, $G = 0$ and:

$$\phi_r(r) = A \frac{e^{-\frac{r}{L_r}}}{r}$$

We can now apply the thin interface boundary conditions since the neutron source shell is considered as thin. The continuity of the flux and current at the interface yields:

$$\begin{aligned}\phi_c(R) &= \phi_r(R) \\ J_{cn}(R) &= J_{rn}(R) + J_{\text{neutron source}}\end{aligned}$$

The flux continuity at the boundary implies:

$$F = A \frac{e^{-\frac{R}{L_r}}}{R}$$

The current boundary condition becomes:

$$\begin{aligned}D_c \nabla \phi_c(R) &= D_r \nabla \phi_r(R) + J_{\text{neutron source}} \\ 0 &= A \frac{D_r}{R} \left[-\frac{e^{-\frac{R}{L_r}}}{R^2} - \frac{1}{L_r R} e^{-\frac{R}{L_r}} \right] + (\eta_{\text{neutron source}} - 1) \Sigma_{aF} A \frac{e^{-\frac{R}{L_r}}}{R} T\end{aligned}$$

The constant A cancels out yielding the critical condition for the assembly as:

$$D_r \left[\frac{1}{R} + \frac{1}{L_r} \right] = T (\eta_{\text{neutron source}} - 1) \Sigma_{aF}$$

SUBCRITICAL NEUTRON MULTIPLICATION

The subcritical multiplication M is defined as:

$$M = \frac{\text{Total neutron flux due to primary source and fissions}}{\text{Neutron flux due to source alone}} \quad (1)$$

To study M let us assume the following:

1. Neutron multiplying medium.
2. Multiplication factor is less than unity corresponding to subcritical multiplication:

$$k_{eff} < 1. \quad (2)$$

3. A source of neutrons: cosmic rays, spontaneous fissions, (α, n) or Po-Be or Ra-Be source is inserted in its center.
4. A control rod can be withdrawn to increase the value of k_{eff} . The effective multiplication factor for a particular assembly under consideration depends upon its size as well as its composition and arrangement.

The number of neutrons after $(m-1)$ generations or neutron lifetimes is:

$$\begin{aligned} n &= n_0 + k_{eff}n_0 + k_{eff}^2n_0 + \dots + k_{eff}^{m-1}n_0 \\ &= n_0(1 + k_{eff} + k_{eff}^2 + \dots + k_{eff}^{m-1}) \\ &= n_0 \frac{1 - k_{eff}^m}{1 - k_{eff}}, m > 0. \end{aligned}$$

After a sufficiently long time:

$$m \rightarrow \infty,$$

and:

$$n = n_0 \frac{1}{1 - k_{eff}} \quad (4)$$

The subcritical multiplication is thus:

$$M = \frac{n}{n_0} = \frac{1}{1 - k_{eff}} \quad (5)$$

When $k_{\text{eff}} = 0.5$, the subcritical multiplication levels off after several neutron lifetimes to a value:

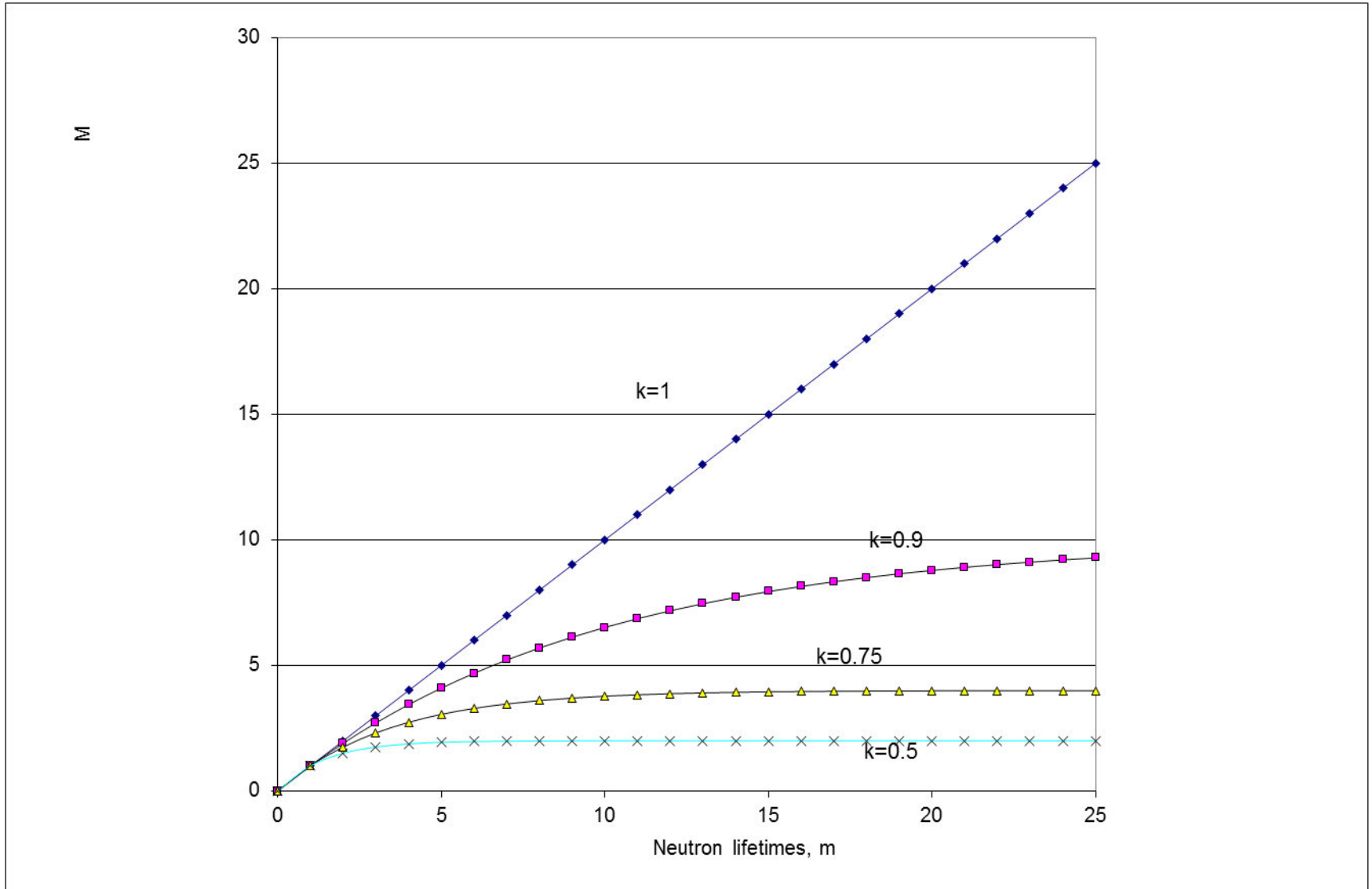
$$M = \frac{n}{n_0} = \frac{1}{1-0.5} = 2.0$$

As k_{eff} approaches unity, the subcritical multiplication factor approaches infinity and the number of neutrons in the medium rises as a straight line with time:

$$M = \frac{n}{n_0} = 1 + 1^2 + 1^3 + \dots + 1^{m-1} = m \quad (6)$$

As the subcritical multiplication becomes higher and higher, more time is taken by the medium to settle at a given level. Finally it does not settle out but continues to rise linearly. If the assembly were supercritical, it would increase exponentially instead.

Subcritical multiplication as a function of the neutron lifetimes. k = effective multiplication factor.



ONE-GROUP FINITE-DIFFERENCE CRITICALITY MODEL

Data for One-Group Diffusion Code

Fission averaged microscopic cross sections from the JENDL3.2 data files

Isotope	σ_a (b)	σ_s (b)	σ_f (b)	ν
U ²³³	2.02	5.645	1.946	2.48
Th ²³²	0.179	7.454	NA	NA
F ¹⁹	0.0208	3.589	NA	NA
B ⁹	0.0944	2.673	NA	NA
Li ⁷	0.02	1.8447	NA	NA
Graphite	0.002	2.363	NA	NA

Core composition and data for fuel salt which yields $k_\infty = 1.00$

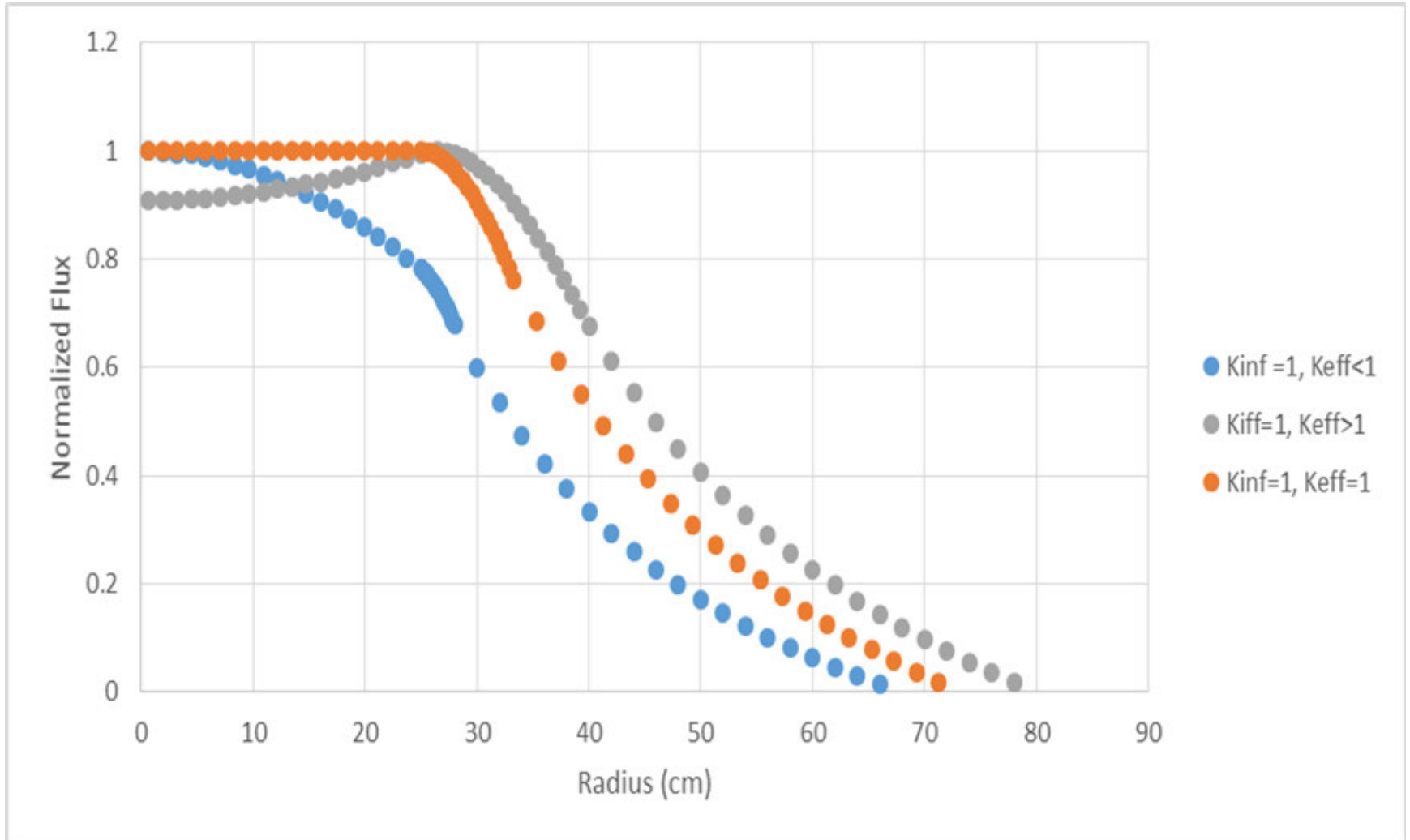
Molten Salt Composition	Density ρ (g/cm ³)	Macroscopic Absorption cross-section Σ_a (cm ⁻¹)	Macroscopic scattering cross section Σ_s (cm ⁻¹)	Macroscopic fission cross-section Σ_f (cm ⁻¹)	$\nu * \Sigma_f$ (n/cm)	Diffusion coefficient D (cm)
16%BeF ₂ – 69%LiF – 12%ThF ₄ – 3% ²³³ UF ₄	4.0345	0.004879	0.288918	0.001968	0.004880	1.1834408

Data for reflector region

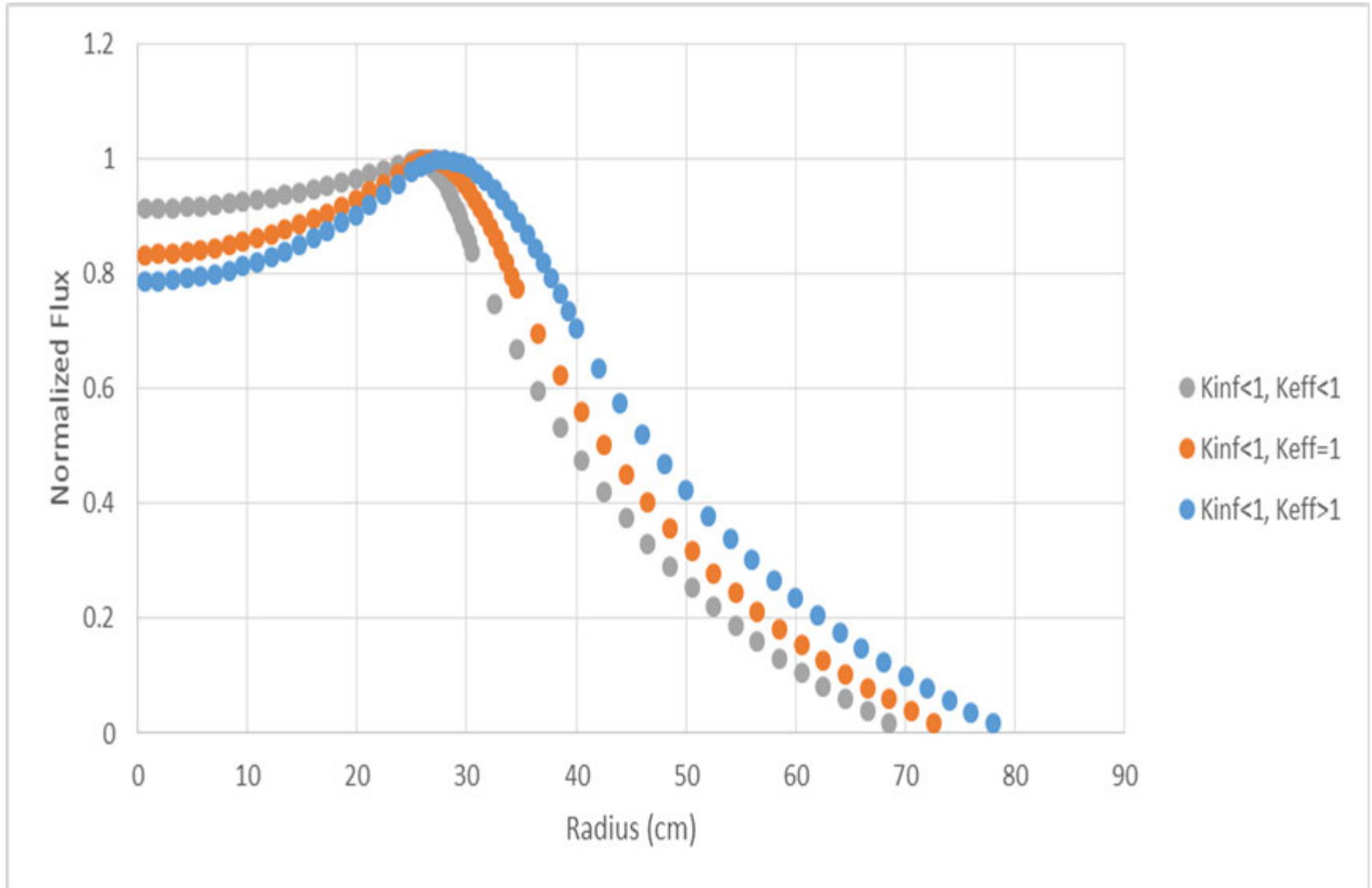
	ρ (g/cm ³)	Σ_a (cm ⁻¹)	Σ_s (cm ⁻¹)	D (cm)
Graphite	2.267	0.000227531	0.268828152	1.311712192

II. NUMERICAL CRITICALITY ANALYSIS

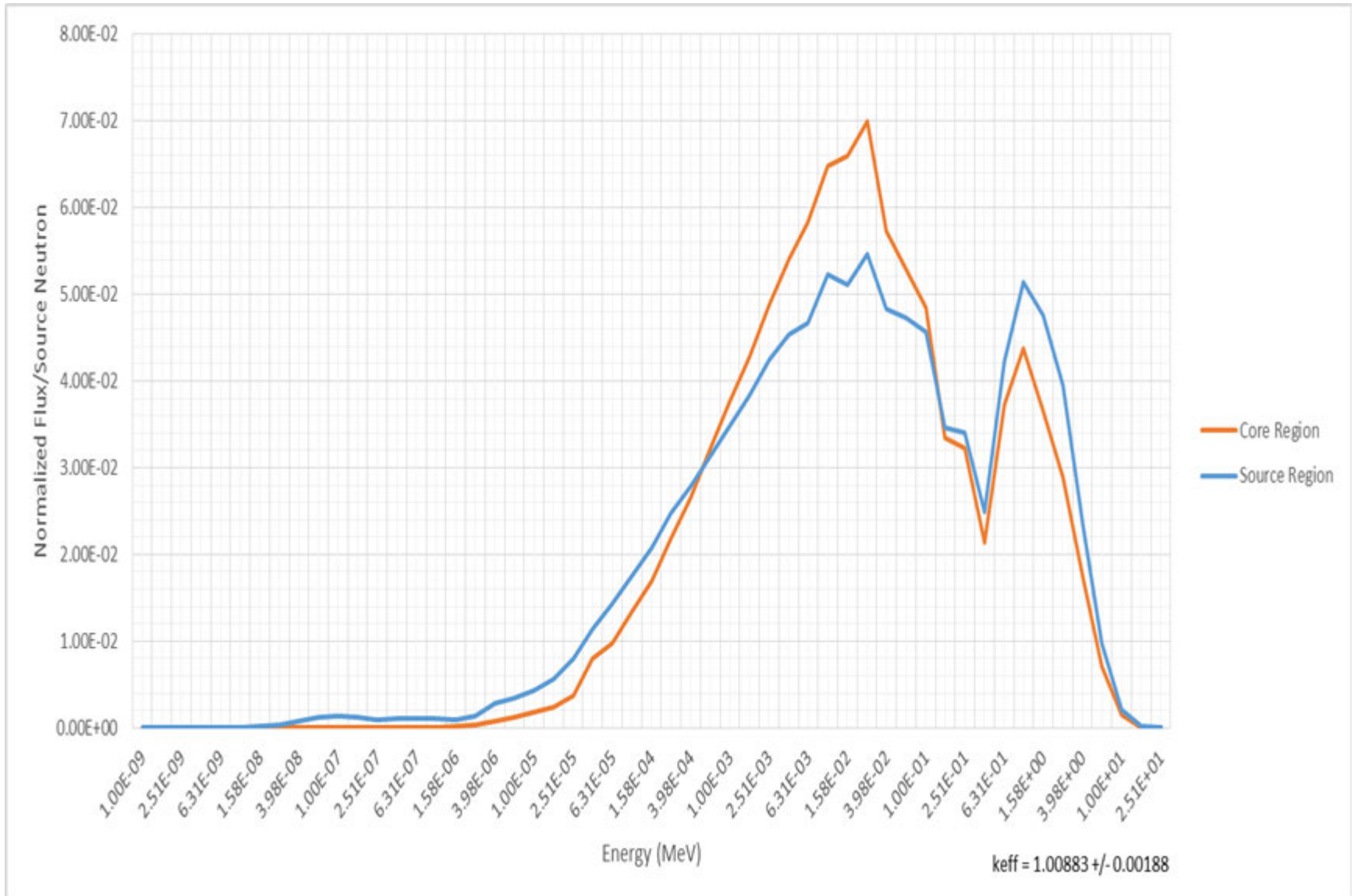
Normalized Flux vs. Radius for Various Criticality Conditions for core with $k_{\infty}=1$



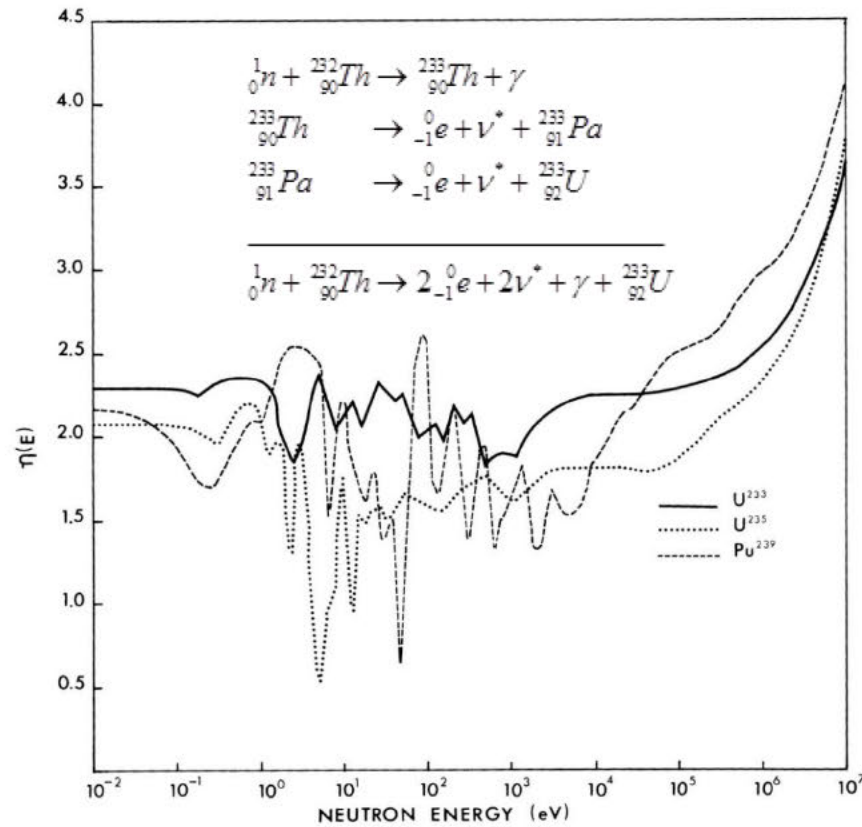
Normalized Flux vs. Radius for Various Criticality Conditions for core $k_{\infty} < 1$



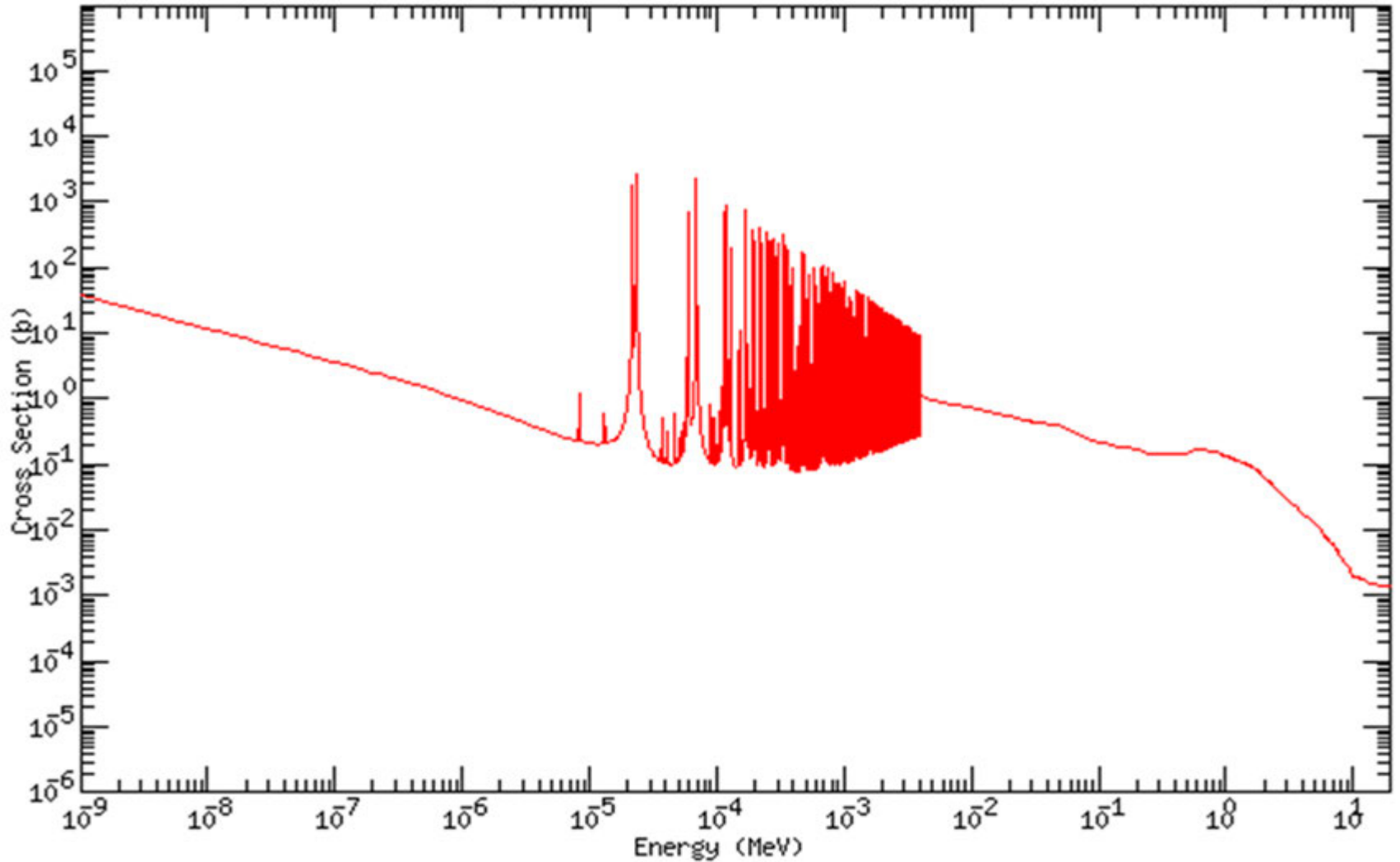
Averaged Neutron Flux Spectra over the Core and Source Regions



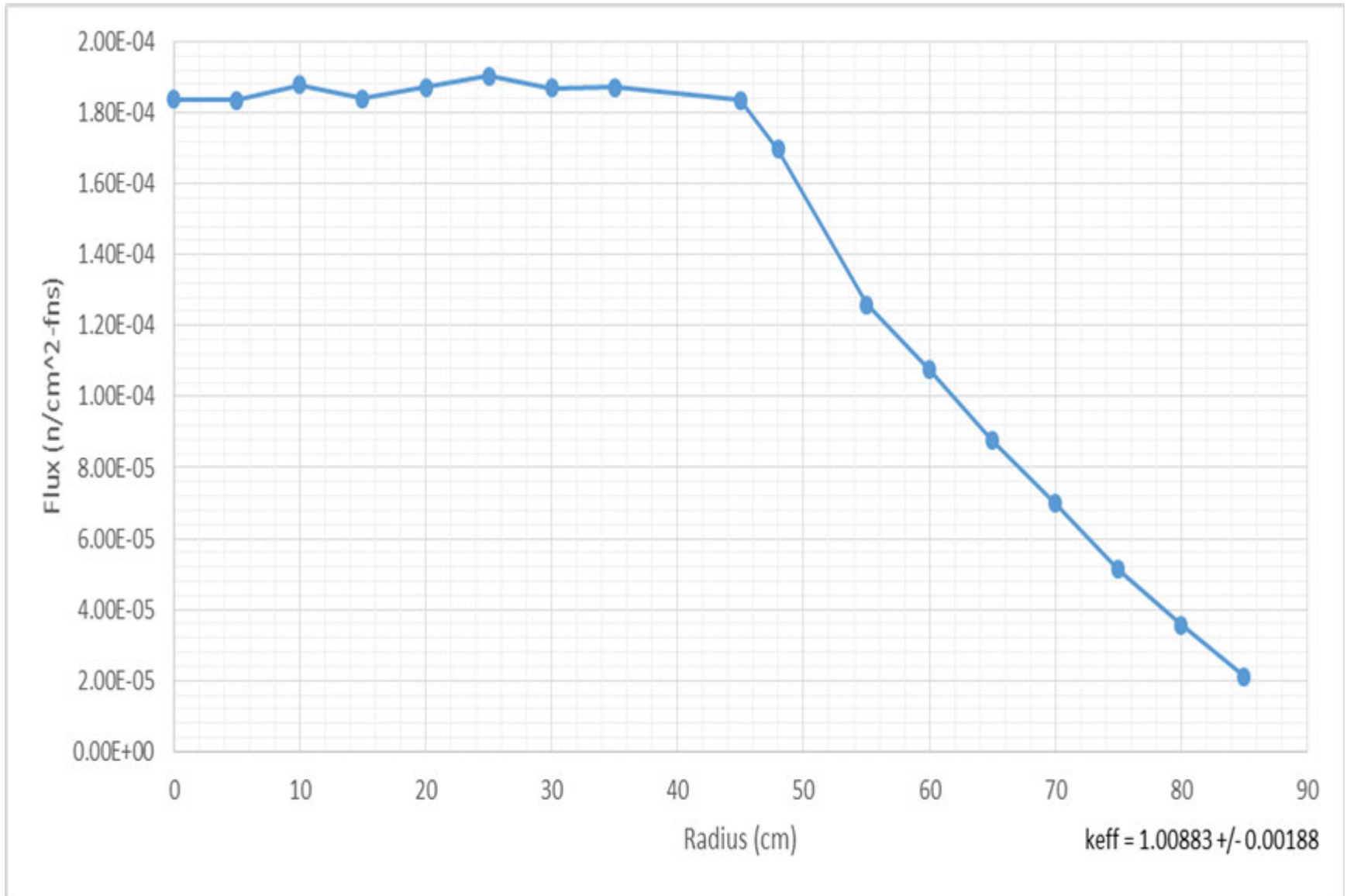
Regeneration factor as a function of neutron energy for the different fissile isotopes. Breeding in the Thorium-U²³³ fuel cycle can be achieved with thermal or fast neutrons.



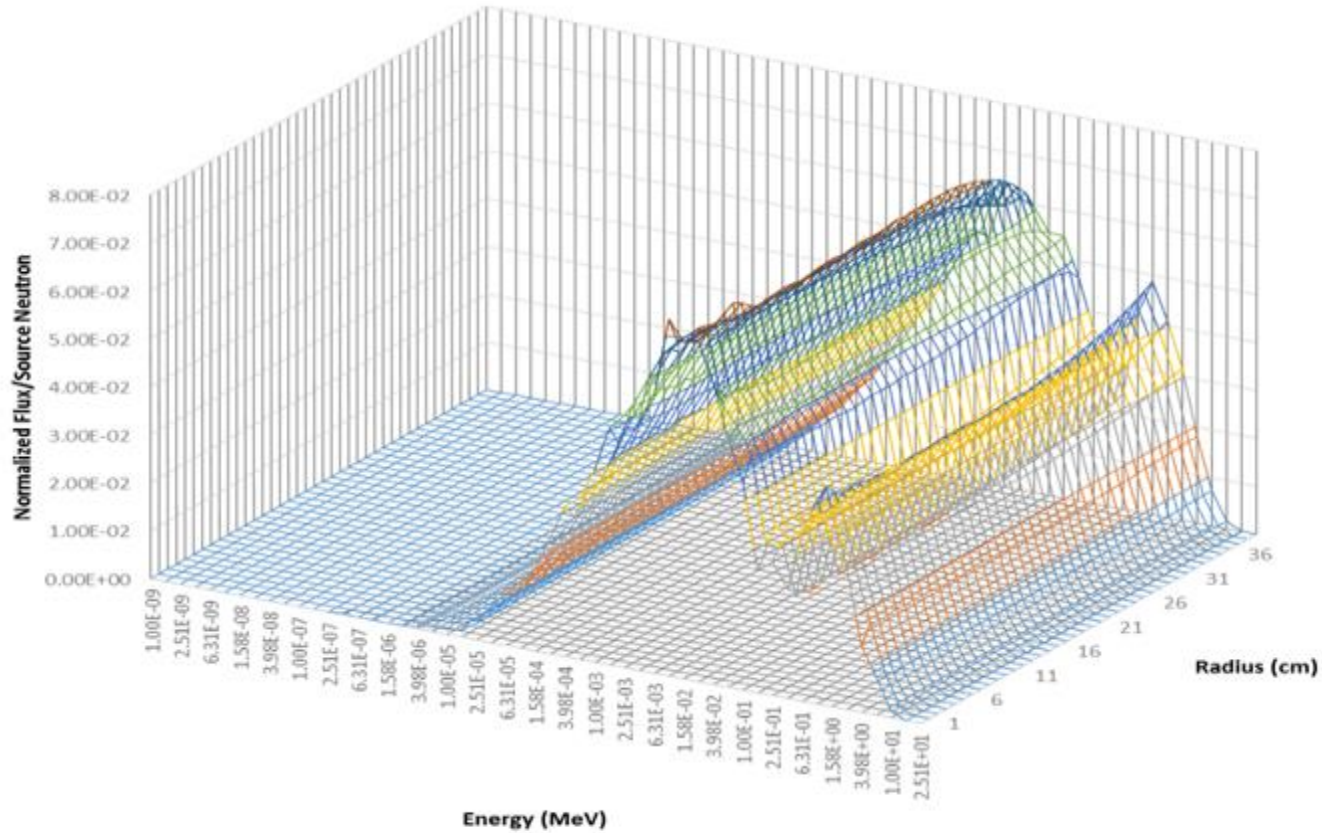
Thorium neutron Radiative Capture Cross Section vs. Energy

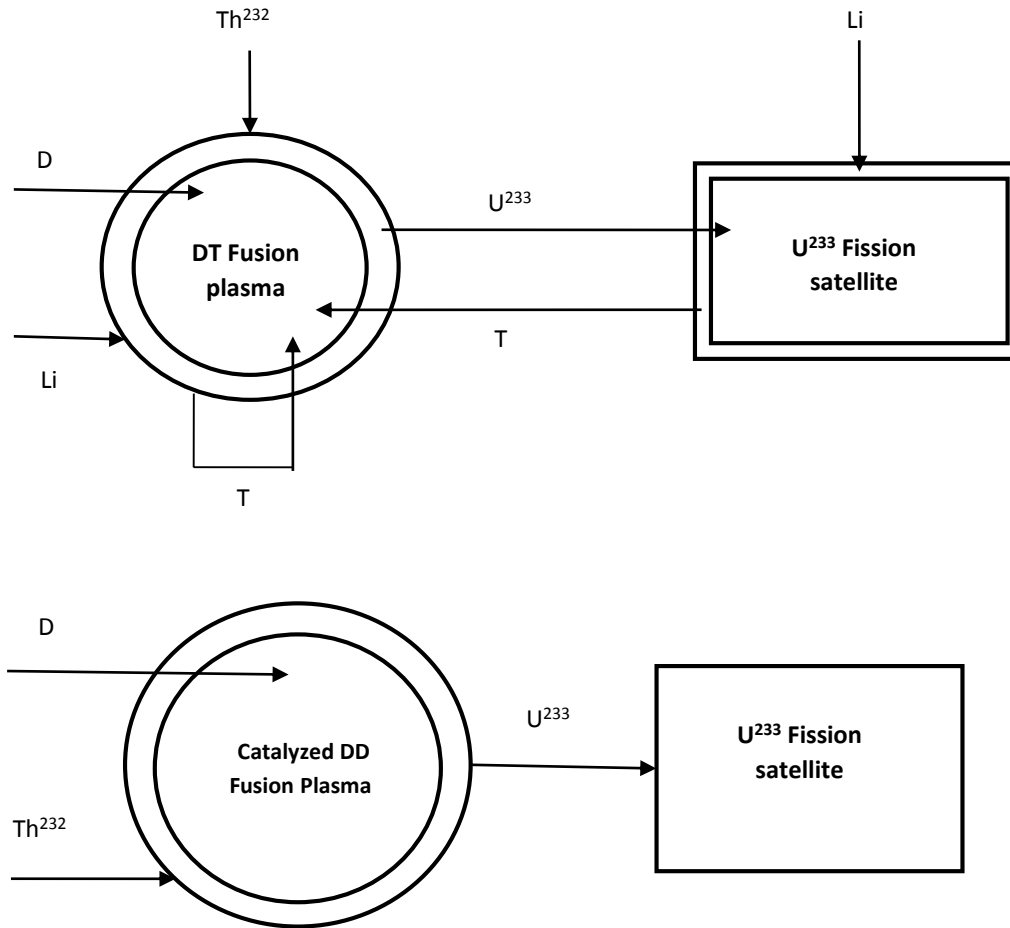


Neutron Flux vs. Radius for Core Surrounded by Fissile Source Region



Average Flux Spectrum over Incremental Radial Sections in Core Region





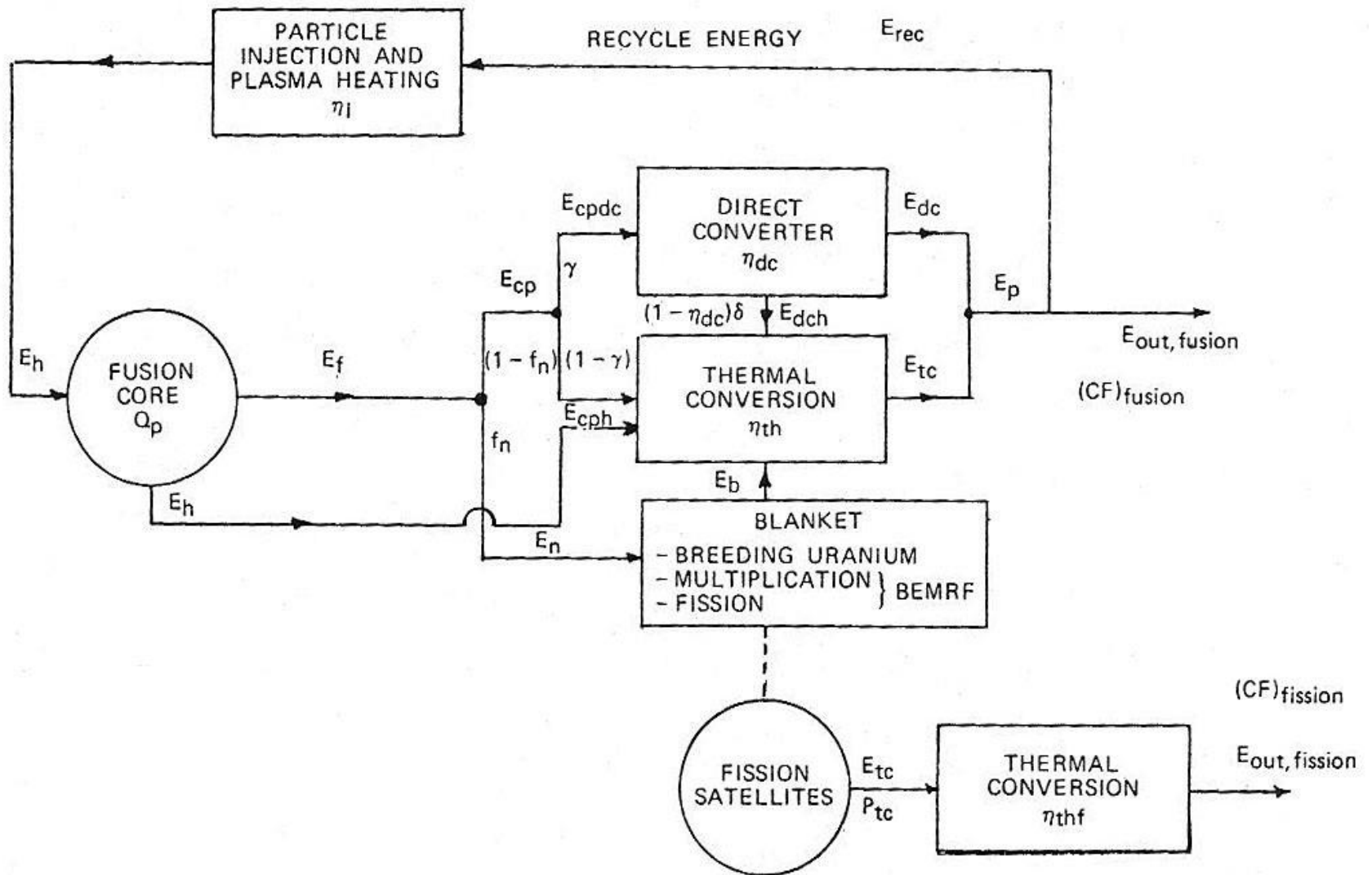
Material flows in the DT (top) and Catalyzed DD fusion-fission hybrid (bottom) Fuel Factory alternatives with U^{233} breeding from Th^{232} .

Catalyzed DD and DT Fusion Reaction Energetics.

Reaction	Total Energy from fusion, E_f (MeV)	Charged Particle Energy (MeV)	Neutron Energy (MeV)	Fraction of energy to neutrons, f_n (%)	Number of Neutrons
DT reaction					
${}_1D^2 + {}_1T^3 \rightarrow {}_2He^4(3.52) + {}_0n^1(14.06)$	17.57	3.52	14.06	80.02	1
Catalyzed DD reaction*					
(a) $\frac{1}{2}{}_1D^2 + \frac{1}{2}{}_1D^2 \rightarrow \frac{1}{2}{}_1T^3(1.01) + \frac{1}{2}{}_1H^1(3.03)$	4.04	4.04	0.00	0.00	0
(b) $\frac{1}{2}{}_1D^2 + \frac{1}{2}{}_1D^2 \rightarrow \frac{1}{2}{}_2He^3(0.82) + \frac{1}{2}{}_0n^1(2.45)$	3.66	2.43	1.23	33.61	1/2
(c) $\frac{1}{2}{}_1D^2 + \frac{1}{2}{}_1T^3 \rightarrow \frac{1}{2}{}_2He^4(3.52) + \frac{1}{2}{}_0n^1(14.06)$	8.79	1.76	7.03	80.02	1/2
(d) $\frac{1}{2}{}_1D^2 + \frac{1}{2}{}_2He^3 \rightarrow \frac{1}{2}{}_2He^4(3.67) + \frac{1}{2}{}_1H^1(14.67)$	9.17	9.17	0.00	0.00	0
-----	-----	-----	-----	-----	---
$3{}_1D^2 \rightarrow {}_2He^4 + {}_1H^1 + {}_0n^1$	21.62	13.36	8.26	38.21	1

DT and DHe³ reactions (c) and (d) proceed at the same rate as the two DD reactions. $R_1 = R_2 = \frac{R_{DD}}{2}$

*DD reactions (a) and (b) are assumed to have a branching ration of ½ and proceed at an equal rate:



SYMBIOTIC COUPLING OF FUSION BREEDERS AND FISSION SATELLITES, ENERGY AND MATERIAL BALANCES

ENERGY AMPLIFICATION FACTOR AND SUPPORT RATIOS

The energy amplification factor or fission to fusion energy multiplication , is then given by

$$= \frac{P_{tc}}{P_f} = \frac{E_{fission}}{E_f} \cdot \frac{U}{(1-C)(1+\alpha)} \cdot \frac{CF_{fusion}}{CF_{fission}} \quad (21)$$

ENERGY AND ELECTRICAL SUPPORT RATIOS

Three figures of merit can be suggested for the assessment of the symbiotic fusion and fission combination.

1. The fission to fusion energy amplification factor defined by Eq. 18. It measures the multiplication of the energy external to the fusion generators in the fission reactors satellites when the bred fissile fuel releases its energy content.

$$= \frac{E_{fission}}{E_f} \cdot \frac{U}{(1-C)(1+\alpha)} \cdot \frac{CF_{fusion}}{CF_{fission}} \quad (21)'$$

The energy amplification is increased at a first level by the factor

$$\frac{E_{fission}}{E_f} = \frac{190}{17.57} = 10.8, \text{ for DT fusion}$$

$$\frac{E_{fission}}{E_f} = \frac{190}{21.62} = 8.8, \text{ for Catalyzed DD fusion}$$

Parameter values for the symbiotic fusion and fission coupling

Parameter	Symbol	Catalyzed DD	DT
Beam injection and plasma heating efficiency	η_I	0.80	0.80
Fraction of fusion energy carried by neutrons	f_n	0.38	0.80
Fusion energy output per fusion reaction (MeV/fusion)	E_f	21.62	17.57
Total blanket energy multiplication	BEMRF	1.38	1.29
Fraction of fusion charged particles energy flowing to direct converter	γ	0.42	0.00
Direct conversion efficiency	η_{dc}	0.80	0.00
Fraction of energy rejected by the direct converter recoverable through thermal conversion	δ	1.00	0.00
Fusion thermal conversion cycle efficiency	η_{th}	0.40	0.40
Fission thermal conversion cycle efficiency	$\eta_{th,fs}$	0.30	0.30
Fusion plant capacity factor	CF_{fusion}	0.60	0.60
Fission plant capacity factor	$CF_{fission}$	0.70	0.70
Energy release per fission event (MeV/fission)	$E_{fission}$	190	190
Capture to fission ratio	α	0.10	0.10
Conversion ratio of converter reactors	C	0.60	0.60
Fissile nuclei yield per source neutron	U	0.880	0.737
Plasma power amplification factor	Q_p	0.01	0.01

A much more drastic contribution can be noticed by the factor: $\frac{1}{1-C}$, where the conversion factor C is defined as

$$C = \frac{\text{average number of fissile nuclides produced}}{\text{average number of fissile nuclides consumed}}$$

As the value of the conversion factor C approaches unity, an infinite energy multiplication factor ensues:

$$\lim_{C \rightarrow 1} = \lim_{C \rightarrow 1} \left[\frac{E_{fission}}{E_f} \cdot \frac{U}{(1-C)(1+\alpha)} \cdot \frac{CF_{fusion}}{CF_{fission}} \right] = \infty$$

In detail, when N nuclei of fissile fuel are consumed, NC nuclei of fertile fuel are converted into fissile nuclei. If the process is repeated, the consumption of N fuel nuclei results in the conversion of a total number of fissile nuclei as:

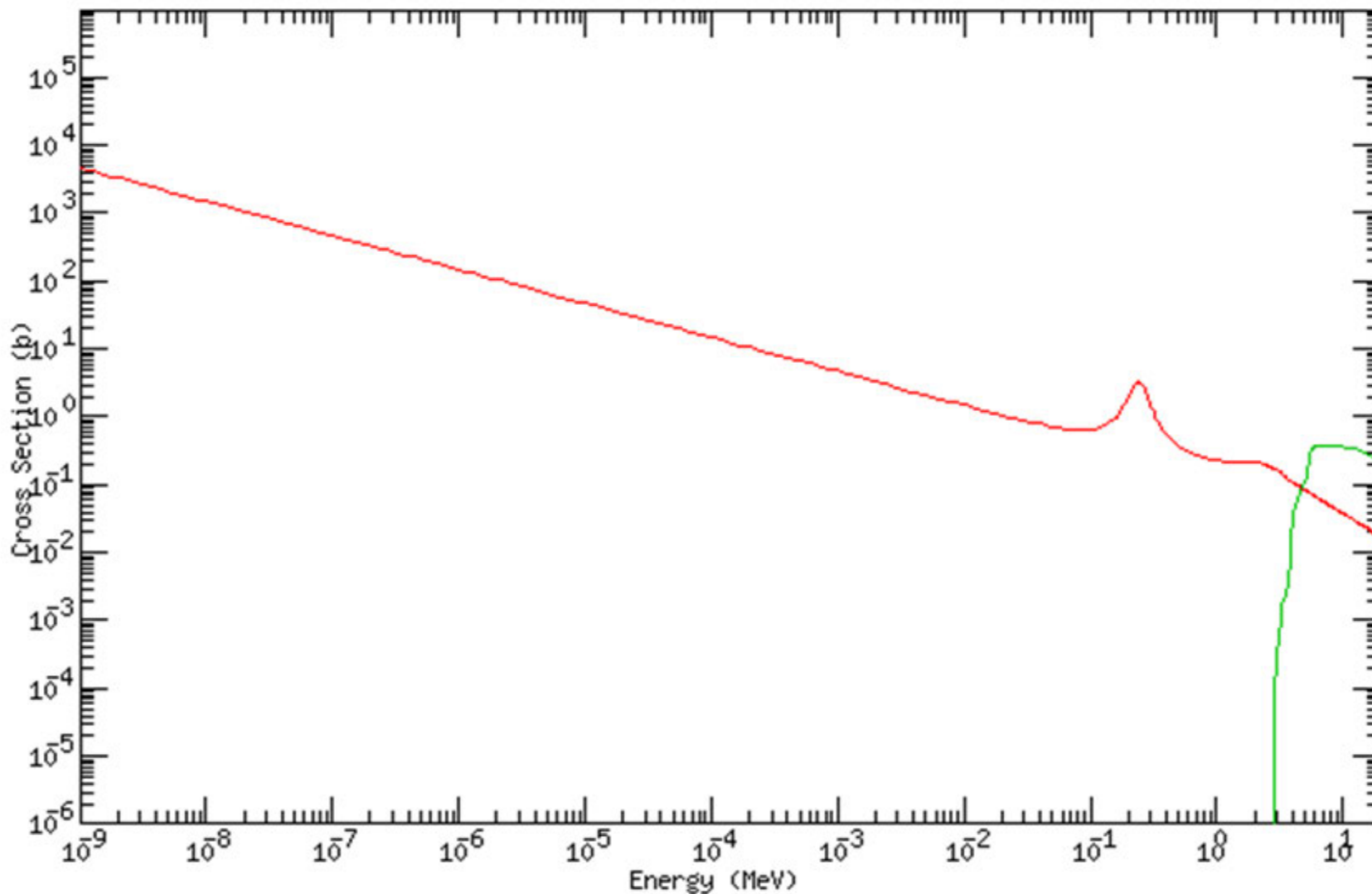
$$\begin{aligned} N_{total} &= N + NC + NC^2 + NC^3 + NC^4 + \dots \\ &= N(1 + C + C^2 + C^3 + C^4 + \dots) \\ &= N \frac{1}{1-C}, \forall 0 < C < 1. \end{aligned} \tag{24}$$

When $C = 1$, an infinite amount of fissile fuel can be converted from a starting amount of fertile fuel. When $C > 1$ the sequence diverges since more than a fissile nucleus is created from a fertile nucleus and cannot be summed mathematically. In this case C is designated as B , the breeding ratio.

If only n recycles are involved, due to the accumulation of undesirable isotopes affecting the recycling process, Eq. 24 reduces to:

$$\begin{aligned}N_{total} &= N + NC + NC^2 + NC^3 + \dots + NC^n \\ &= N(1 + C + C^2 + C^3 + \dots + C^n) \\ &= N \frac{1 - C^{n+1}}{1 - C}, \forall 0 < C < 1.\end{aligned}$$

Tritium Breeding Cross Sections for ${}^6_3\text{Li}$ (red) and ${}^7_3\text{Li}$ (green)



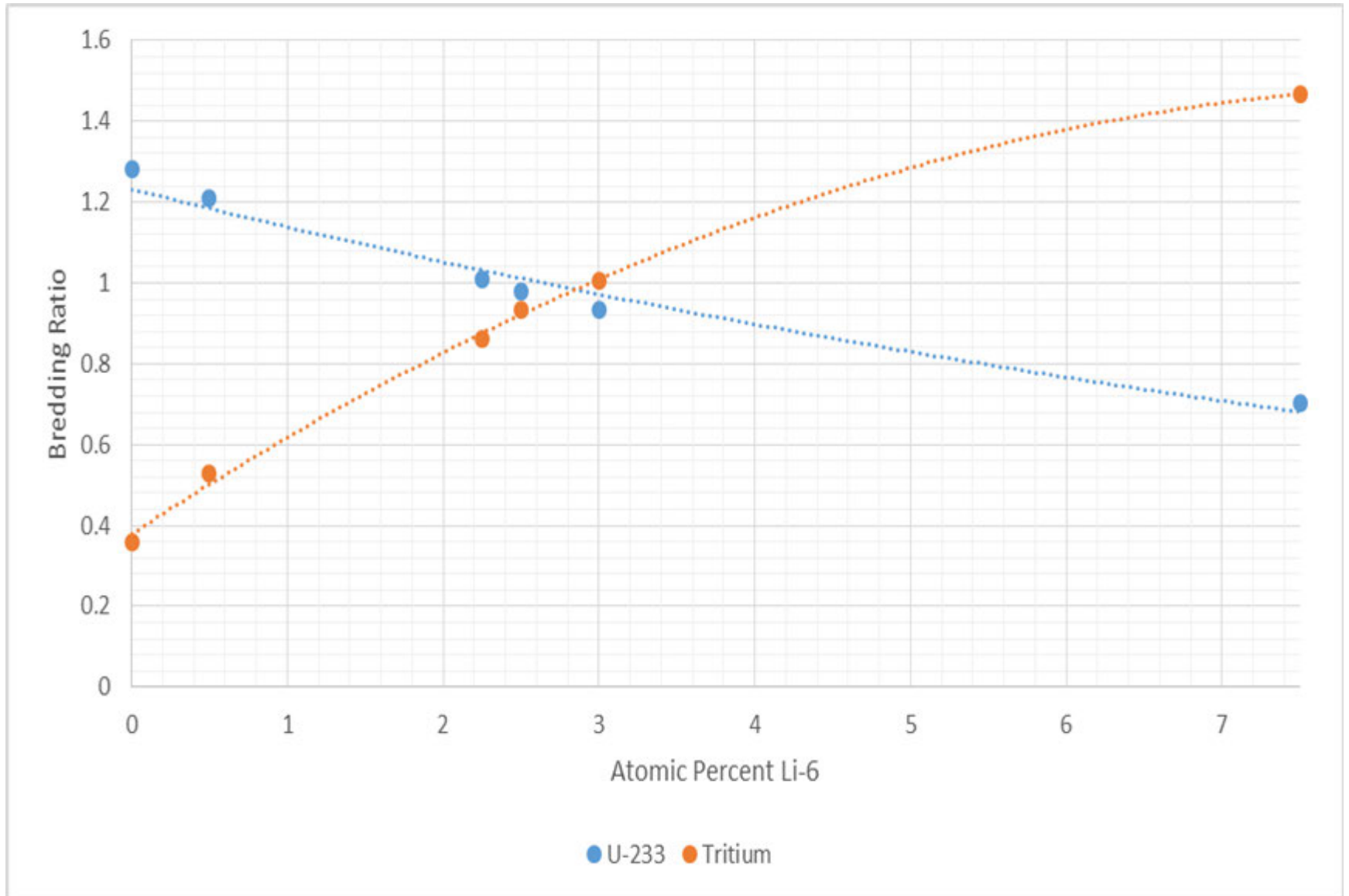
Fail-Safe Reactor Monte Carlo MCNP5 results

	Composition	Mass (kg)	Volume (L)	Density (g/cm ³)	Heat Rate (MeV/fns)	Fission Rate (#/fns)	Fissile Production Rate (#/fns)
Core Region	16% BeF ₂ – 71.02% LiF – 12% ThF ₄ – 0.98% UF ₄	1037.9	268.1	3.872	25.4	0.134	0.197
Fissile Source Region	31% BeF ₂ – 67.9% LiF – 1.1% UF ₄	671.8	265.2	2.533	47.8	0.272	NA

DT driven reactor MCNP results for different ${}^6\text{Li}$ concentrations

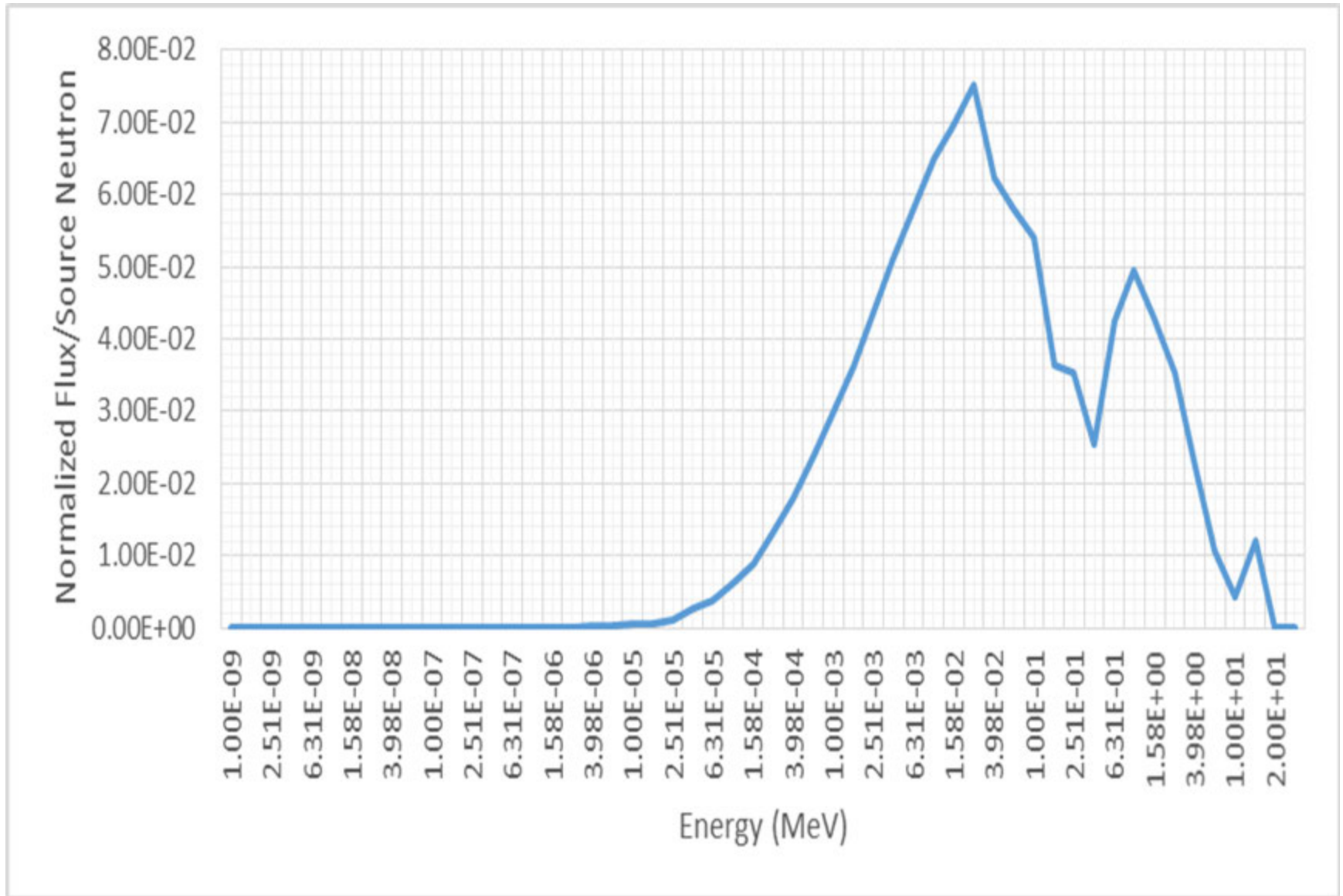
	Composition	Mass (metric tonne)	Volume (L)	Density (g/cm^3)	Heat Rate (MeV/fns)	Fission Rate ($\#/\text{fns}$)	Fissile Production Rate ($\#/\text{fns}$)	Tritium Production ($\#/\text{fns}$)
0% Li-6	16% BeF_2 – 71.02% LiF – 12% ThF_4 – 0.98% UF_4	10.3	2650.7	3.872	294.28	1.57	2.01	0.36
0.5% Li-6	16% BeF_2 – 70.85% LiF – 12% ThF_4 – 1.15% UF_4	10.3	2650.7	3.890	246.69	1.31	1.58	0.53
2.25% Li-6	16% BeF_2 – 70.38% LiF – 12% ThF_4 – 1.62% UF_4	10.4	2650.7	3.925	231.47	1.28	1.28	0.89
2.5% Li-6	16% BeF_2 – 70.32% LiF – 12% ThF_4 – 1.68% UF_4	10.4	2650.7	3.934	244.32	1.29	1.26	0.93
3% Li-6	16% BeF_2 – 70.2% LiF – 12% ThF_4 – 1.8% UF_4	10.4	2650.7	3.940	245.59	1.30	1.22	1.00
NA Li-6	16% BeF_2 – 69.35% LiF – 12% ThF_4 – 2.65% UF_4	10.6	2650.7	4.0095	267.68	1.42	1.00	1.47

Fissile and Fusile Breeding vs. ${}^6\text{Li}$ Concentration

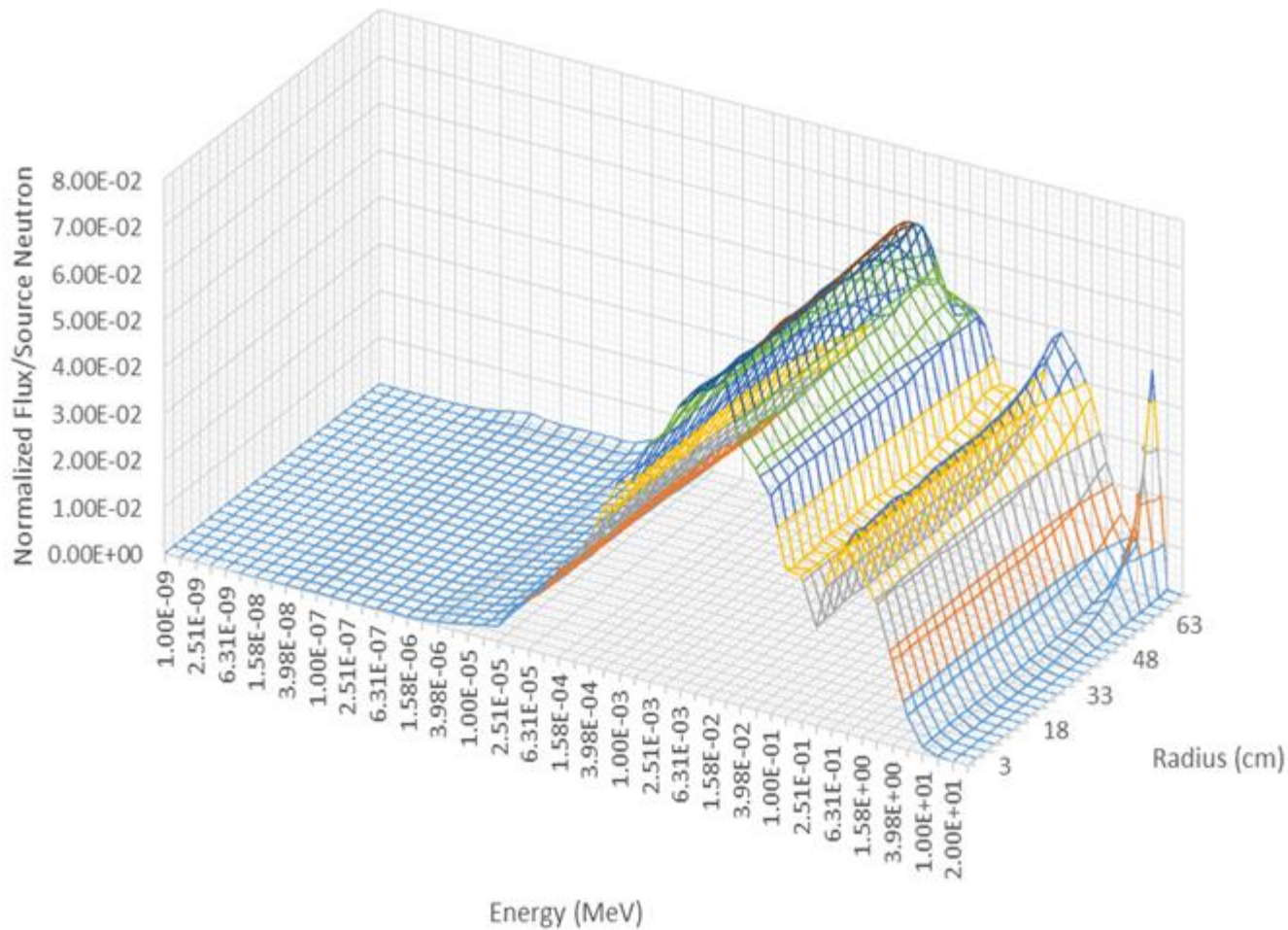


MONTE CARLO POINT CROSS SECTIONS ANALYSIS

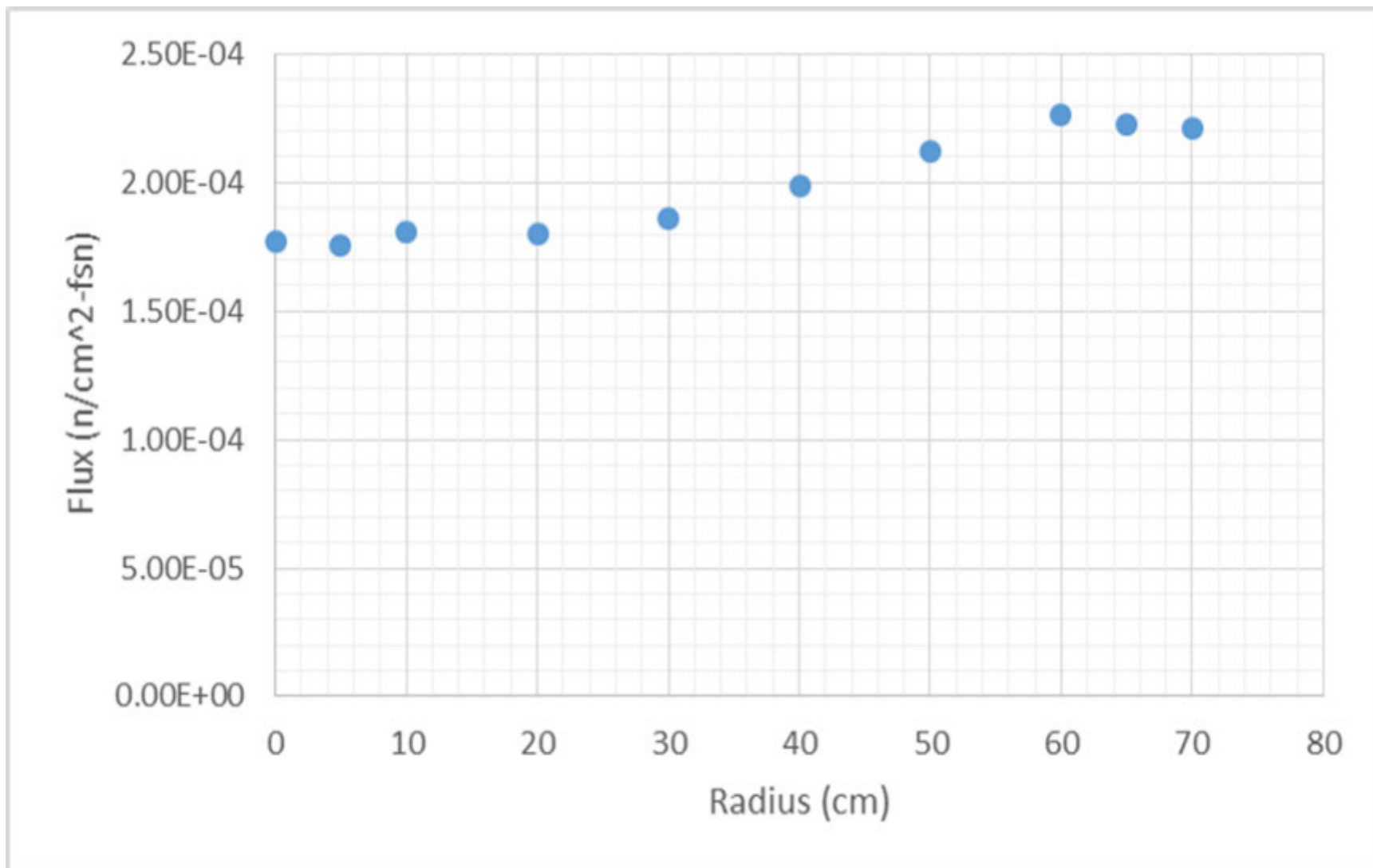
Flux Averaged Over the Core for DT fusion neutron source



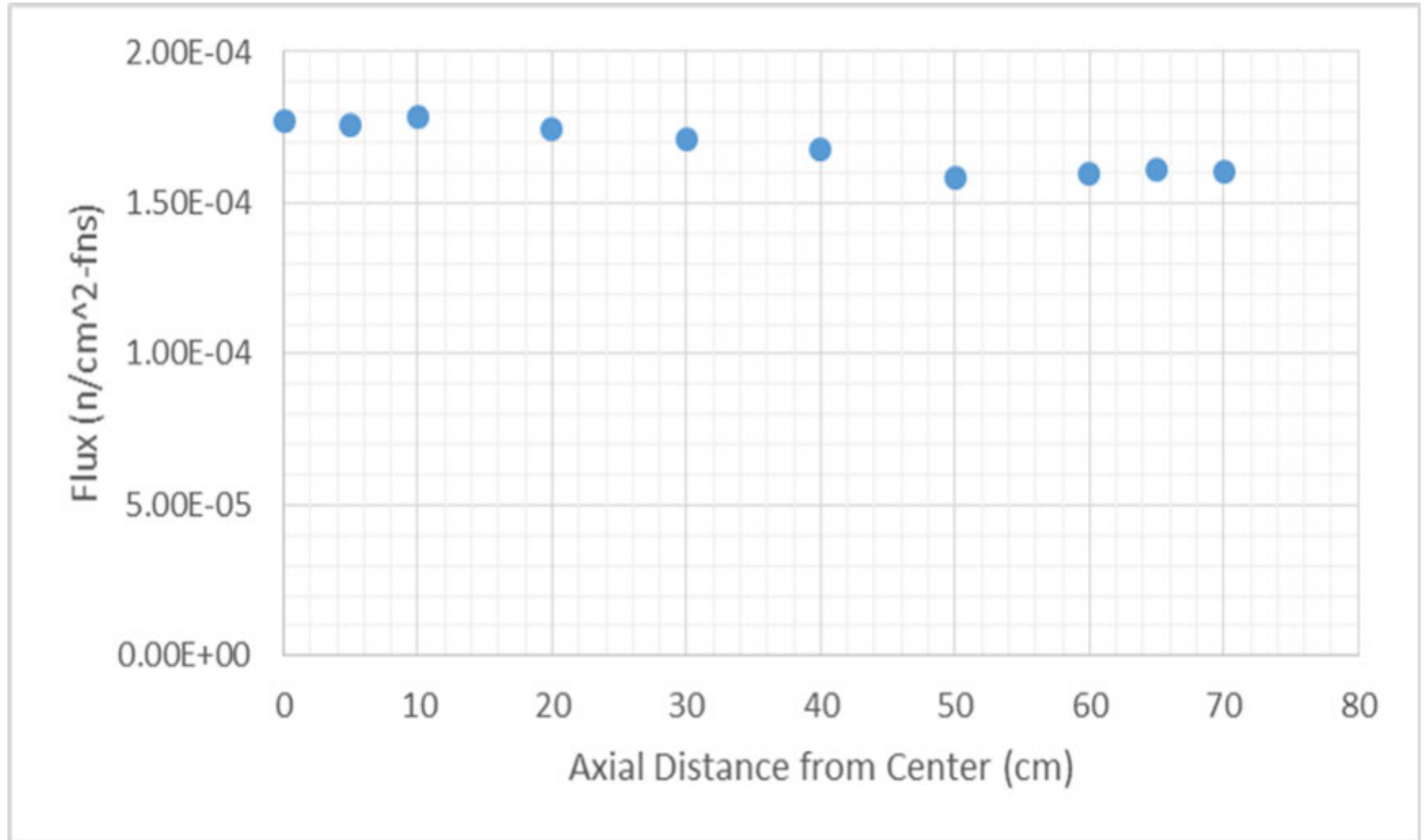
Flux Spectrum over Incremental Radial Sections for DT fusion 14.06 MeV neutron source



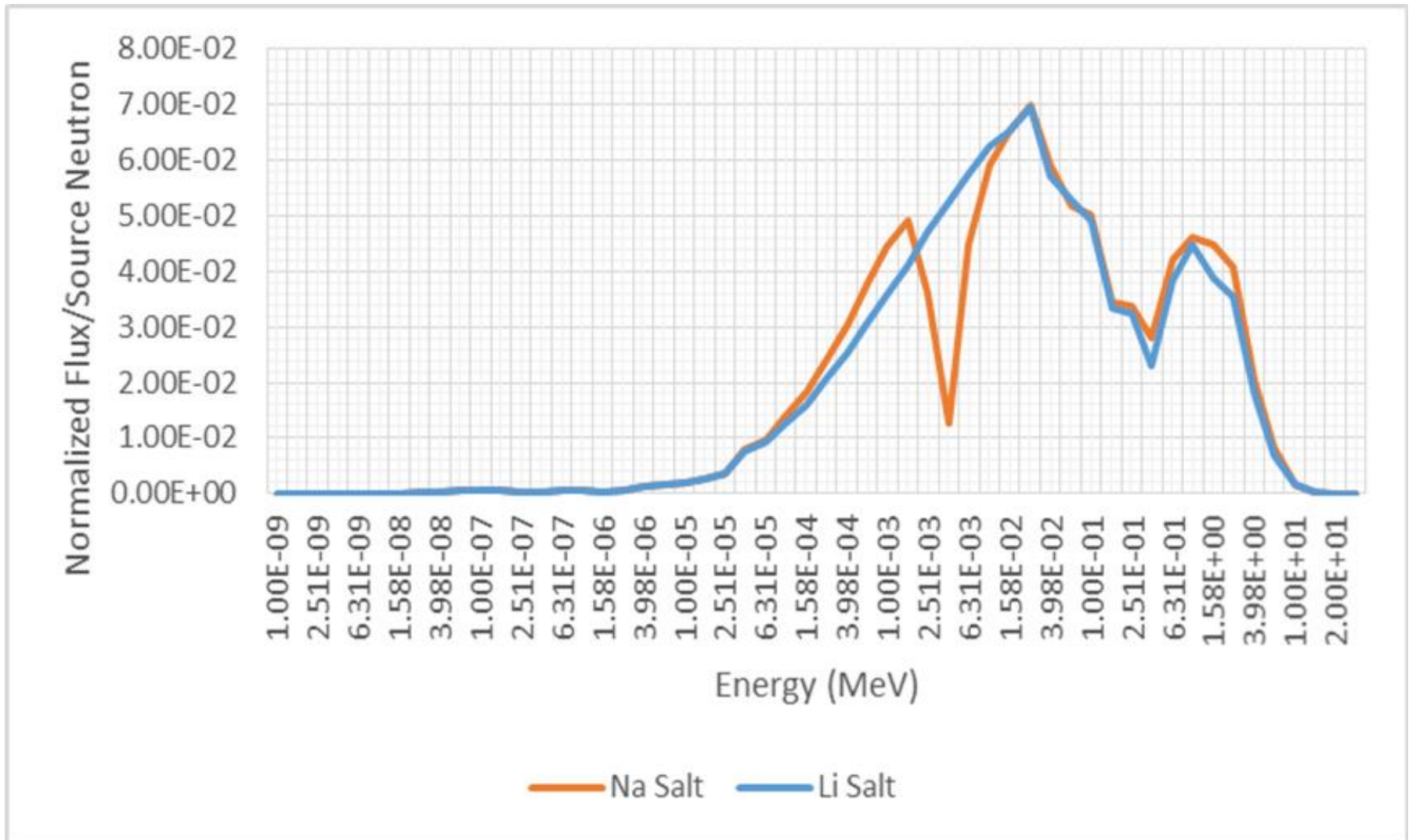
Radial Flux Profile for DT System



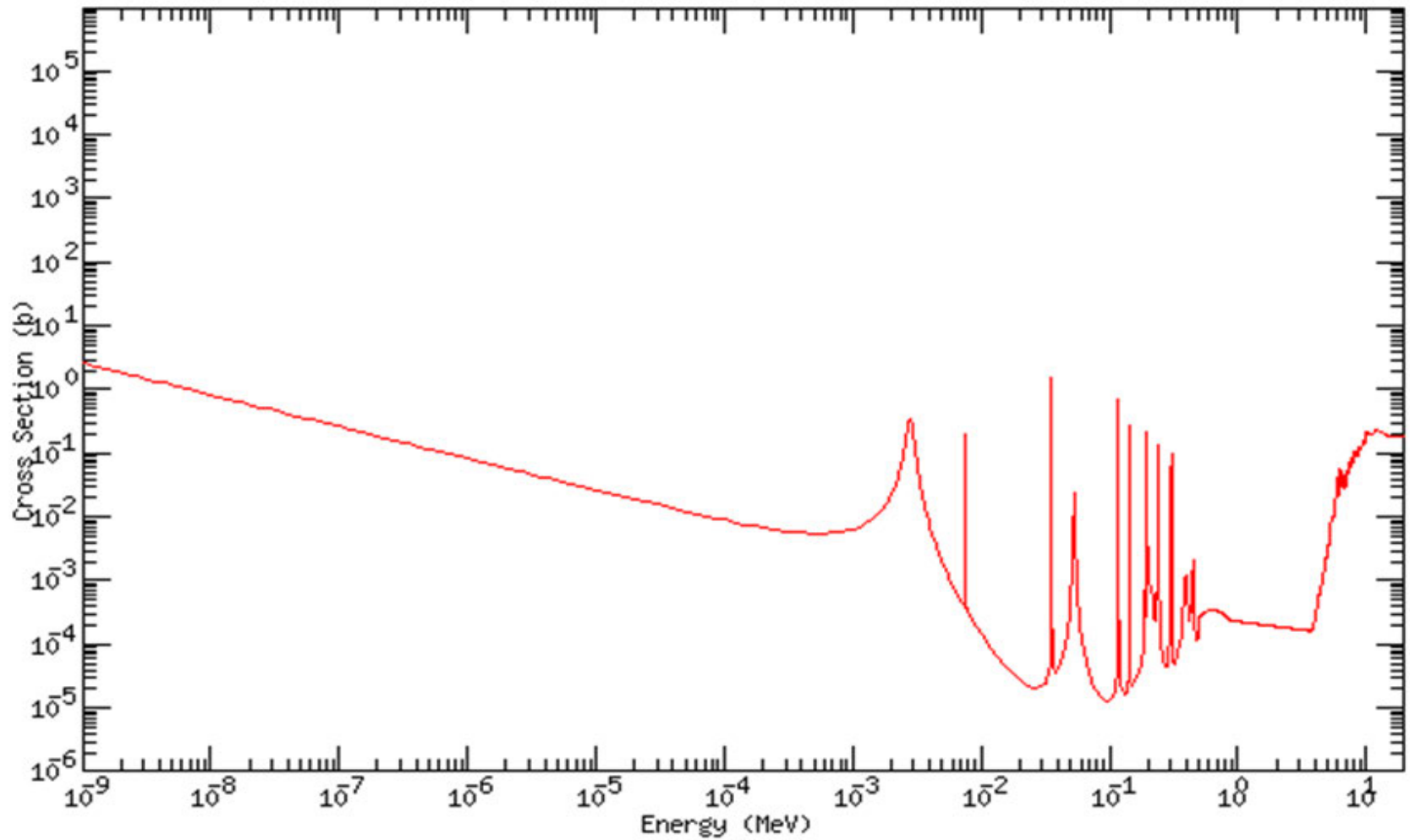
Axial Flux Profile for DT System



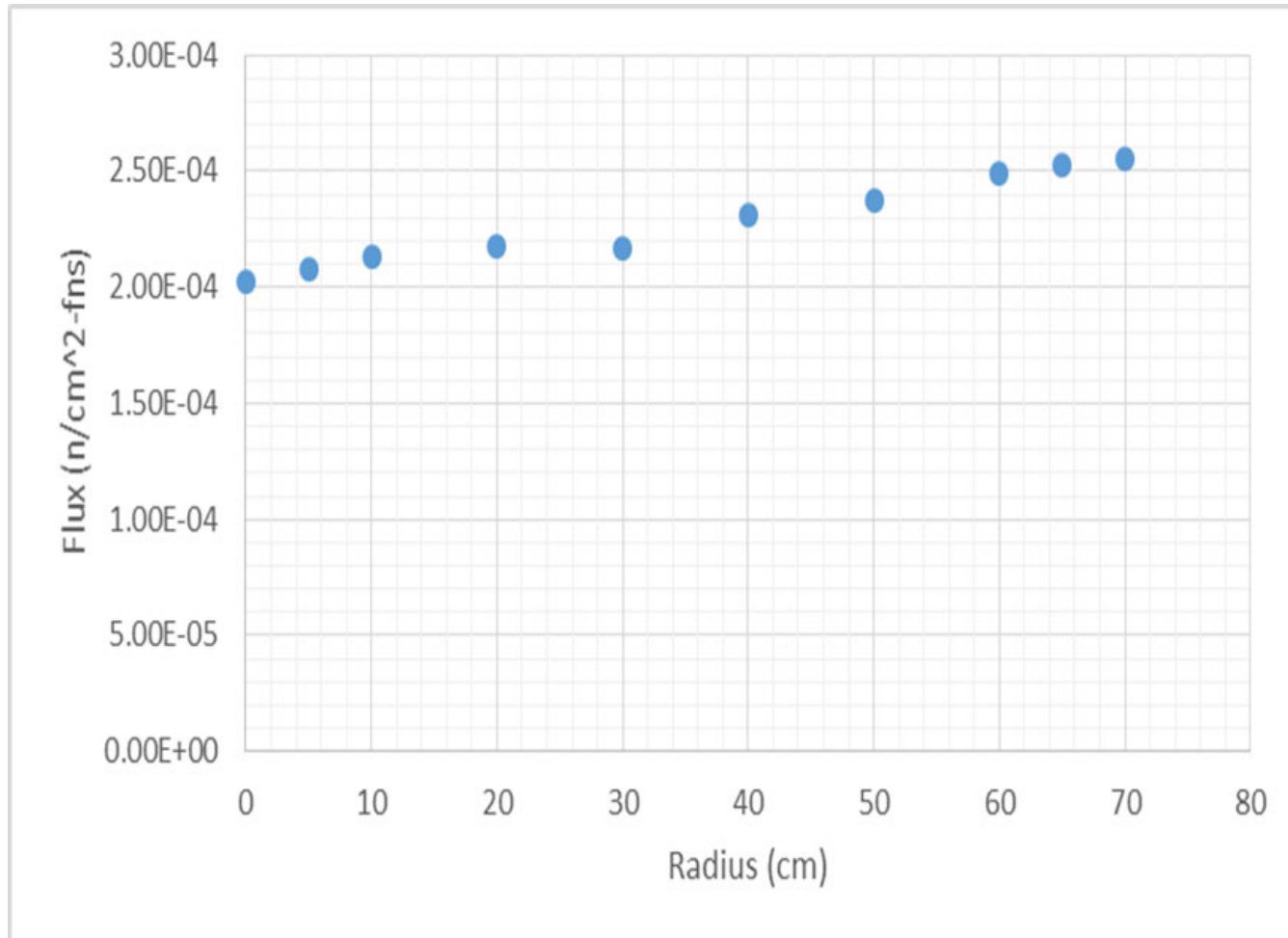
Flux Averaged Over the Core Region of the Li and Na Salt Systems



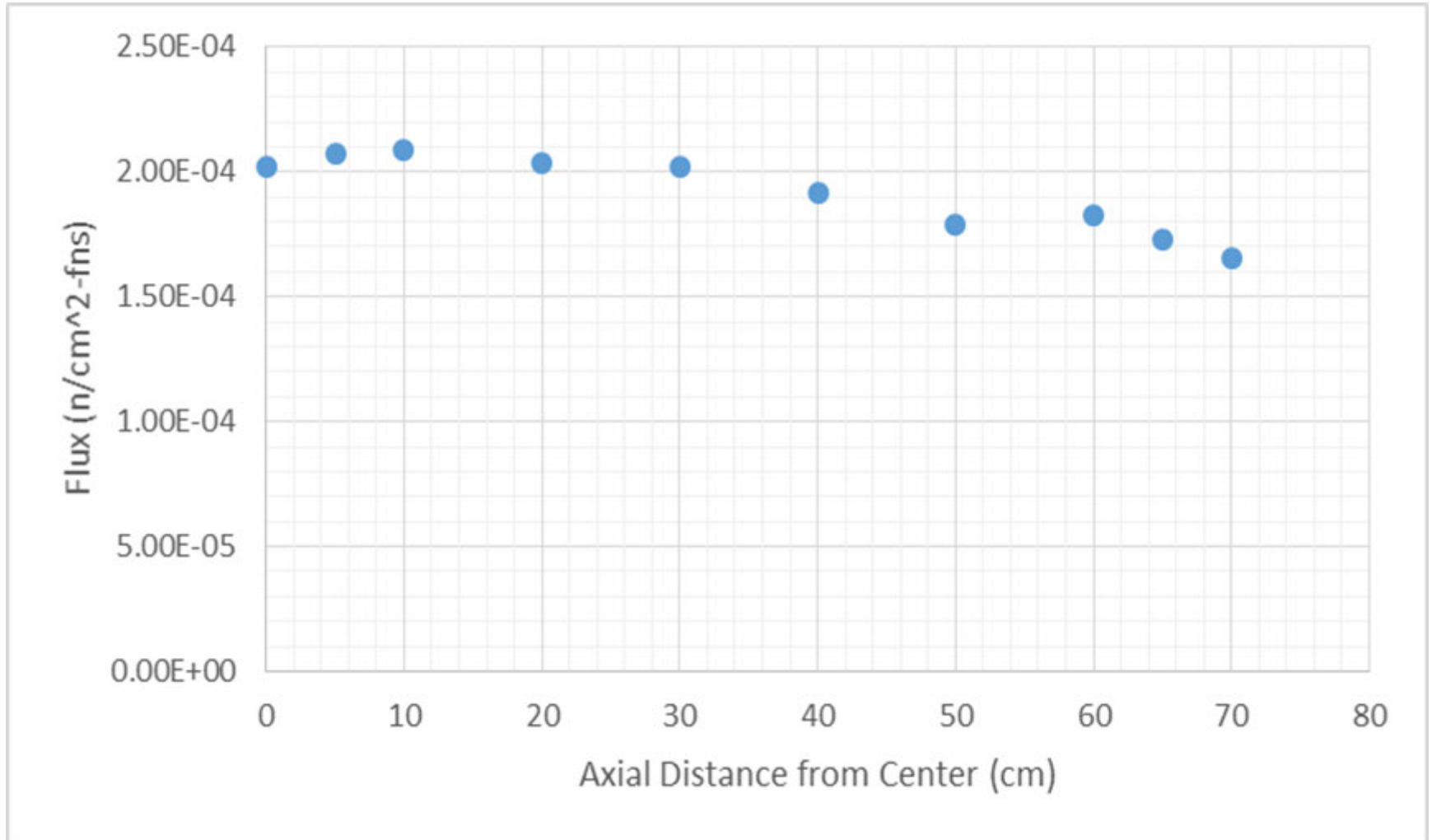
Na neutron absorption cross-section as a function of energy



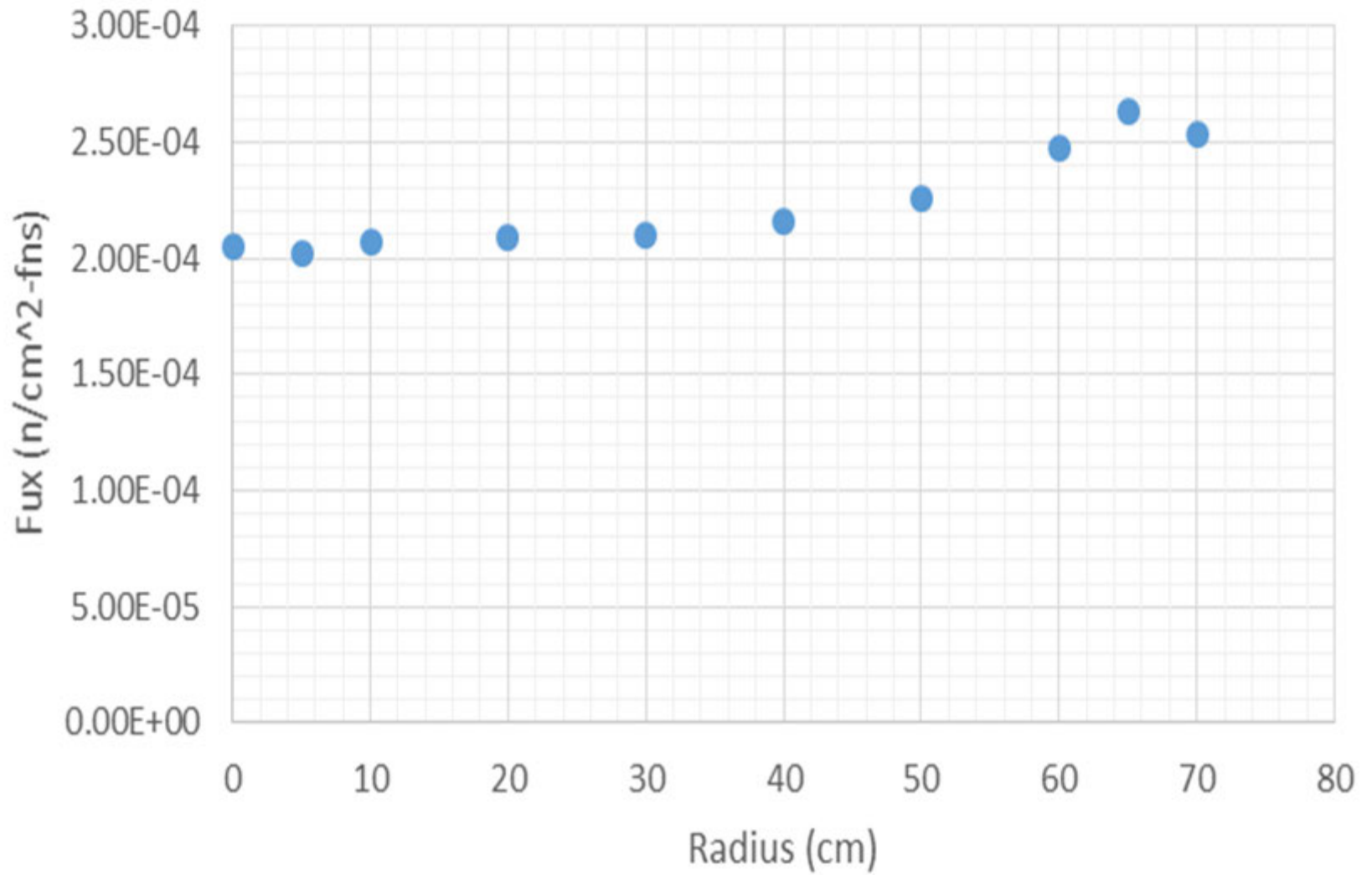
Radial Flux Profile for Na System



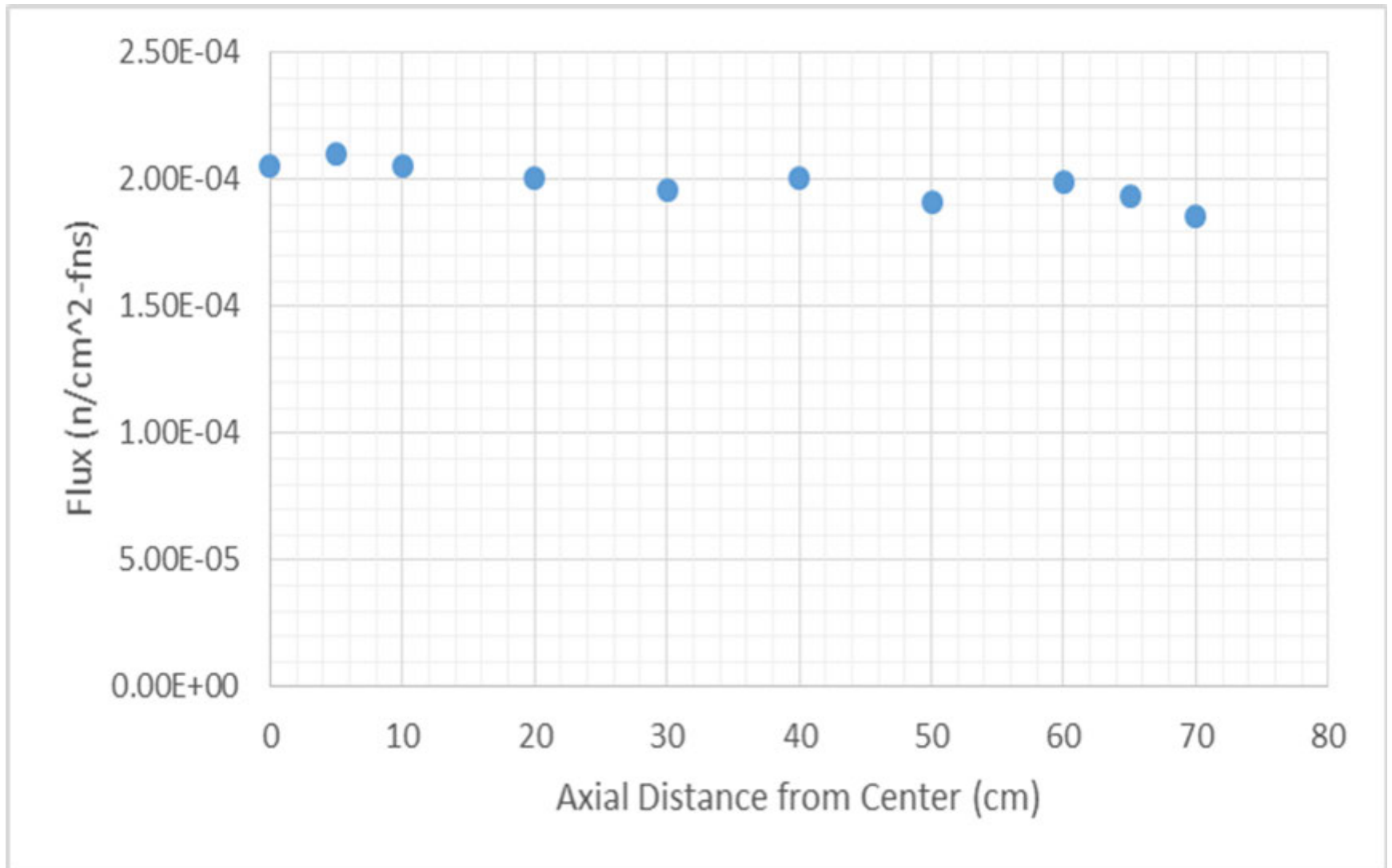
Axial Flux Profile for Na System



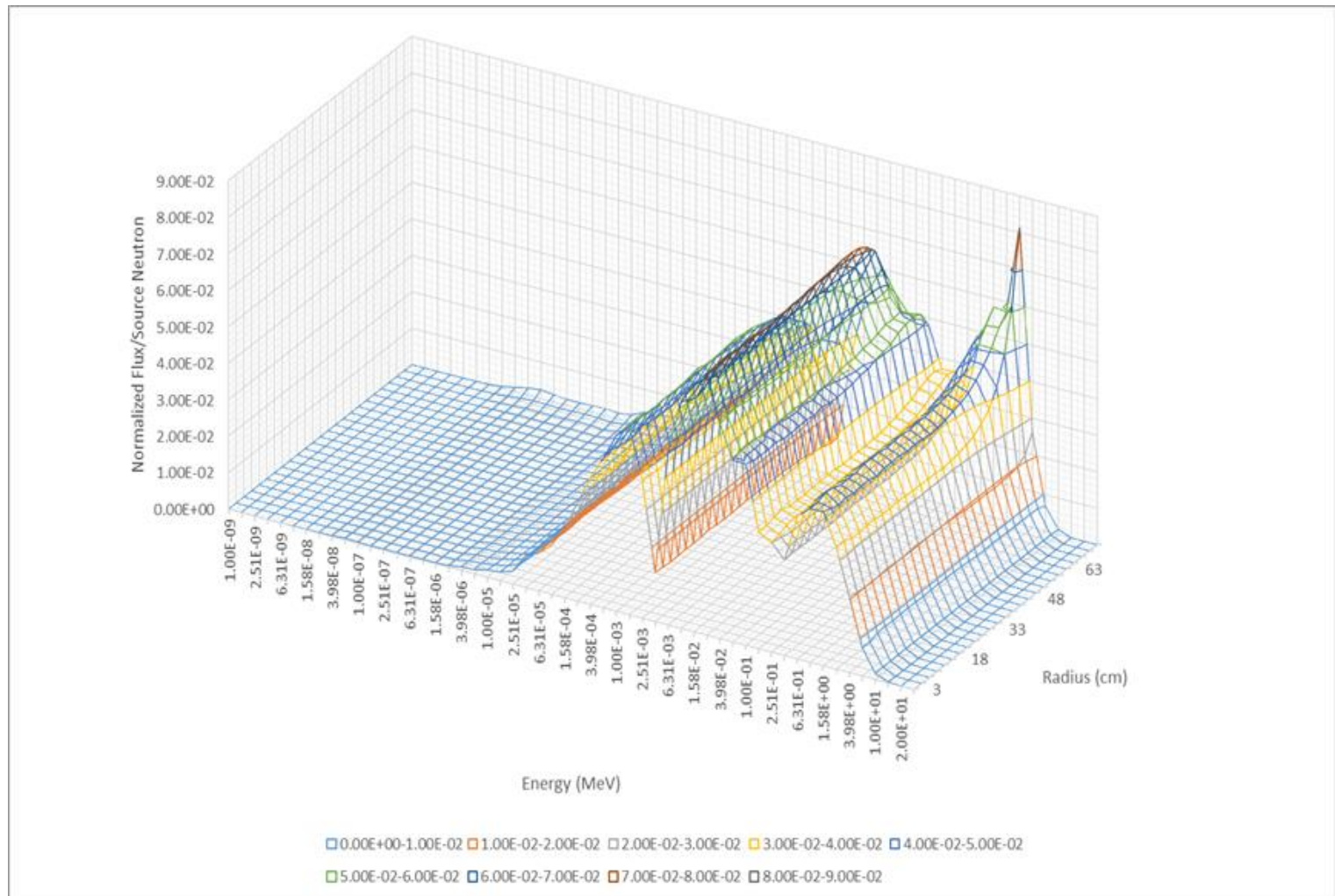
Radial Flux Profile for Li System



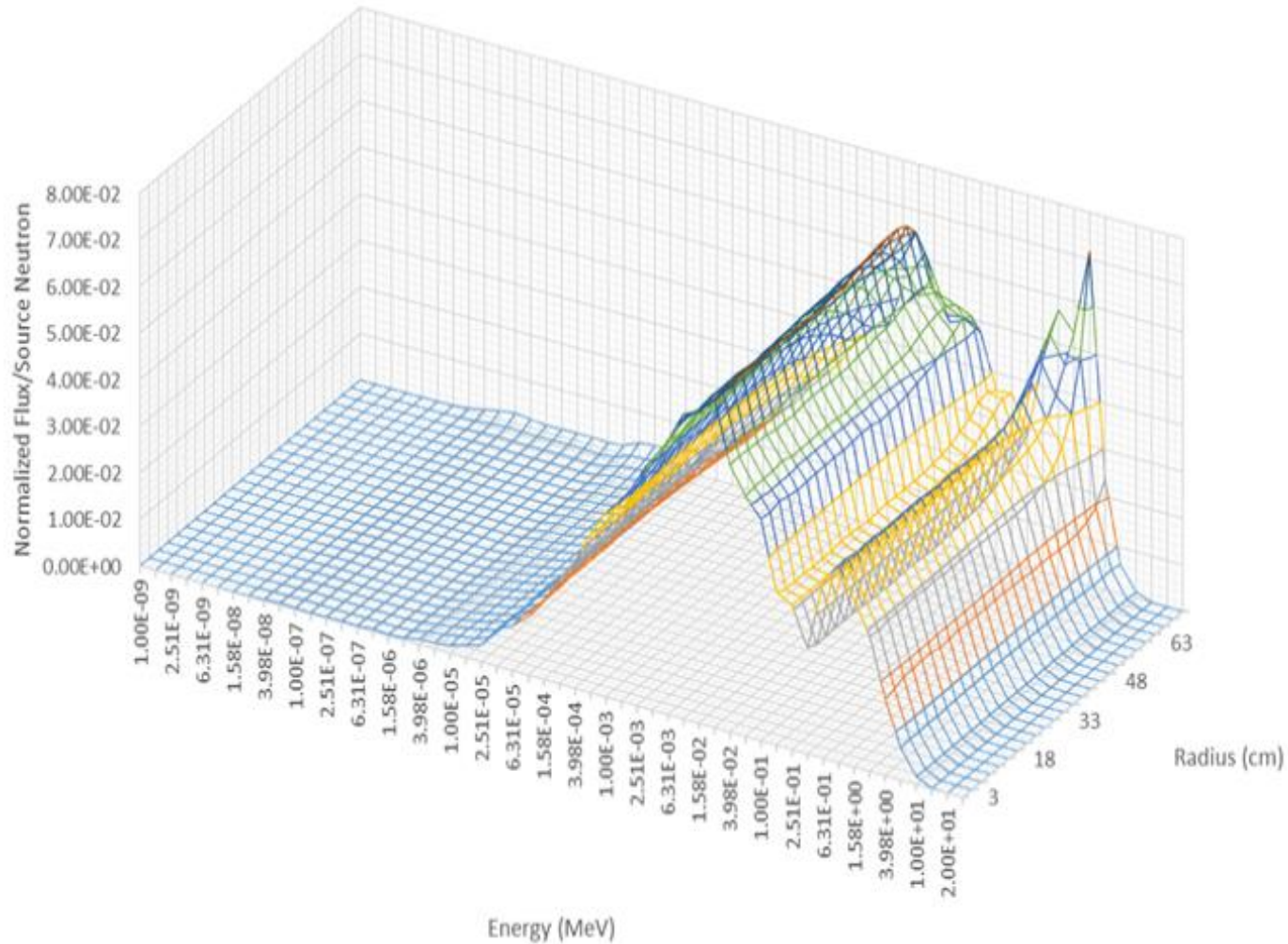
Axial Flux Profile for Li System



Neutron Flux Spectrum over Incremental Radial Sections in Na System



Neutron Flux Spectrum over Incremental Radial Sections in Li System



DD driven reactor MCNP results for different types of salts

	Composition	Mass (tonnes)	Volume (L)	Density (g/cm ³)	Heat Rate (MeV/fns)	Fission Rate (#/fns)	Fissile Production Rate (#/fns)
Li Salt	16% BeF ₂ – 71.02% LiF – 12% ThF ₄ – 0.98% UF ₄	10.3	2650.7	3.872	292.67	1.57	2.00
Na Salt	16% BeF ₂ – 70.94% NaF – 12% ThF ₄ – 1.06% UF ₄	9.45	2650.7	3.565	251.28	1.35	1.70

Computed results of fusion driven systems

System	Composition	M_{net}	k_{eff}	$k_{\text{eff}}^{\text{FS}}$	Source Strength [n/s]	Source Power [MW _{th}]	Net Fissile Production Rate [kg/yr]	Doubling Time [yr]	Fusion Neutron Wall Load (MW/m ²)	BEMR
DT Li	16% BeF ₂ – 70.38% LiF – 12% ThF ₄ – 1.62% UF ₄	3.0888 (+/-) 0.0080	0.88332 (+/-) 0.00281	0.776	7.92E18	22.3	0	NA	3.15	16.5
DD Li	6% BeF ₂ – 71.02% LiF – 12% ThF ₄ – 0.98% UF ₄	3.3706 (+/-) 0.0091	0.90225 (+/-) 0.00034	0.798	6.72E18	7.9	35.2	10.2	1.12	119.5
DD Na	16% BeF ₂ – 70.94% NaF – 12% ThF ₄ – 1.06% UF ₄	3.0642 (+/-) 0.0036	0.88526 (+/-) 0.0017	0.775	7.70E18	9.0	32.9	9.2	1.27	102.6

Monte Carlo Simulation Power Estimates

The spectrum for the reactor is adequate for breeding ^{233}U .

The total energy per fission source in cell one is 25.4 MeV and 47.8 MeV in cell two. Limiting the power density to 120 kW/L, each region can produce up to 32 MW.

Since the source region has a higher heating rate, this means that the core region will have a lower power.

$$N = \frac{32 \text{ [MW]}}{47.8 \left[\frac{\text{MeV}}{n} \right] * 1.602 \times 10^{-13} \left[\frac{\text{J}}{\text{MeV}} \right]} = 4.2\text{E}18 \text{ n/s}$$

$$4.2\text{E}18 \text{ n/s} = \frac{P_{\text{core}} \text{ [MW]}}{25.4 \left[\frac{\text{MeV}}{n} \right] * 1.602 \times 10^{-13} \left[\frac{\text{J}}{\text{MeV}} \right]} = 17 \text{ MW}$$

The neutron rate calculated from is $4.2E18$ n/s and the total power for the system would be $49 \text{ MW}_{\text{th}}$.

The fission rate in the core is 0.134 per neutron source. Conversely, the $\text{Th}(n,\gamma)$ reaction rate is 0.197 per neutron source.

Taking the ratio of fissile production to consumption, yields 1.4 for the breeding ratio in the core.

The fission rate in the source region is 0.272 per source neutron. Thus, the entire system is not breeding, but has a conversion ratio of 0.49 .

The system can be driven in a subcritical state with a fusion neutron source.

DD DRIVEN FAIL-SAFE REACTOR

The DD driven system utilizes the same geometry as the DT driven system. Because the DD driven system does not require tritium, lithium in the salt can be replaced by sodium.

The DD system with a lithium salt is composed of 16% BeF_2 – 71.02% ${}^7\text{LiF}$ – 12% ThF_4 – 0.98% UF_4 , while the sodium salt is composed of 16% BeF_2 – 70.94% NaF – 12% ThF_4 – 1.06% UF_4 . Compositions for the different salts were chosen to such that the $k_\infty = 1$ and the $k_{\text{eff}} \leq 0.90$.

The neutron flux spectra for the two fuel salts have peaks at 25 keV and 1 MeV, while the sodium salt appears to have an additional peak at 1.58 keV. However, this additional peak is actually caused by sodium's large absorption cross section at around 3 keV. Aside from sodium's preferential absorption at around 3 keV, the two salts produce a remarkably similar flux spectrum.

From the MCNP output, the net multiplication in the sodium salt is 3.0642 versus 3.3706 for lithium. The $k_{\text{eff}}^{\text{FS}}$ for the sodium system is 0.775 and 0.798 for the lithium system. The sodium system has a lower heat rate at 251.28 MeV per source neutron versus 292.67 MeV per source neutron. This is attributable to the higher fission rate in the lithium system, as the ratio of the heat rate to fission rate for both systems is the same. Keeping the power of the DD system the same as the DT system, 318 MW_{th} , the required fusion source strength is 6.72E18 n/s for the Li salt and 7.20E18 n/s for the Na salt.

DISCUSSION

1. Molten Salt Reactors (MSRs) offer a great deal of stability compared to their solid fuel counterparts. MSR's are designed with a salt plug drain below the reactor vessel. The plug must be actively cooled and in the case of a loss of power accident or if the fluid becomes too hot, the salt plug will melt and the molten salt will drain into a passively cooled containment vessel capable of removing the decay heat from the system. Furthermore, molten salts have a very strong negative temperature and void coefficients.

2. Another advantage of molten salt systems is the ability to process the fuel during plant operation to remove fission products hence eliminating the decay heat problem. To remove the uranium from the salt, the fluoride volatility process can be utilized. Hydrogen fluoride and then F_2 gas is bubbled through the salt. The uranium is converted from UF_4 to UF_6 and is released from the salt as a gas. The UF_6 is then converted back to UF_4 as needed. This method is also applicable to higher actinides such as plutonium. Fission products can also be removed by several methods such as vacuum distillation or liquid bismuth reductive extraction. Gaseous fission products, such as xenon and krypton are continuously removed by sparging the salt with helium gas. This ability to remove fission products and adjust the fissile concentrations in the salt during operation allows one to maintain stable reactivity and removes the need for burnable poisons. A single control rod can be included for start-up and shutdown but is not necessary due to the ability to drain fuel out the core and into criticality safe storage tanks.

3. The reactor configurations detailed in this workoffer even greater fail-safe safety features than traditional MSRs. In the source-driven fail-safe reactor, the extra fissile material surrounding the core offers greater flexibility in reactivity control, as the core and source salt fissile concentrations can be varied during operations to maintain optimal conditions.

4. Furthermore, the core cannot achieve criticality without the source region material present. This is because the core is at $k_{\infty} = 1$ and therefore $k_{\text{eff}} < 1$ due to neutron losses. Without the source region, the fail-safe reactor modeled earlier would have a $k_{\text{eff}} = 0.61365 \pm 0.00045$.

5. The fusion source driven systems are subcritical. This makes criticality accidents not possible, since the effective multiplication factor k_{eff} is not near 1. Additionally, reactivity can be easily controlled by varying the source strength. Without the source present, the system cannot maintain criticality, making the system stable and fail-safe.

ABSTRACT

A source-driven nuclear reactor configuration with a unity infinite medium multiplication factor fission core is investigated for both fission and fusion-fission hybrid systems. Such configuration is thought to offer a desirable fail-safe reactor alternative in that the loss of the fission or the fusion neutron sources would automatically lead to a shut-down of the system into a stable subcritical state with an effective multiplication factor of less than unity. This is so since the fission core cannot maintain criticality without the presence of the neutron source.

A circulating liquid molten salt using the Th-U²³³ fuel cycle, where the fission products are continuously extracted, further contributes to the fail-safe characteristic by avoiding the cooling needed for the decay heat or afterheat after reactor shut-down. Through the extraction of the Pa²³³ relatively long-lived precursor isotope, and allowing it sufficient time to decay into its U²³³ daughter, breeding in either thermal or fast neutron spectra is a distinct possibility. The presence of trace amounts of U²³² and the strong gamma-emitting Tl²⁰⁸ daughter isotope offers a desirable non-proliferation characteristic for the cycle.

As a proof of principle, a simplified analytical one-group neutronics analysis is first attempted for the pure fission core system. An energy and material flows analysis conducted to estimate the support ratios in a coupled fusion-fission hybrid system, where the bred U²³³ fissile fuel is fed from a fusion-fission fuel factory to pure fission satellites, suggests that sufficient support ratios can be obtained if a conversion ratio that is close to unity can be obtained for the fission island in the coupled system.

This is then supplemented with numerical one-group criticality calculations using an iterative finite-difference methodology. Further, a more detailed multi-group Monte Carlo neutronics analysis of the fission core reactor driven by a U²³³ fission neutron source, Deuterium-Tritium (DT) and Deuterium-Deuterium (DD) fusion neutron sources was conducted using the MCNP5 computer code.

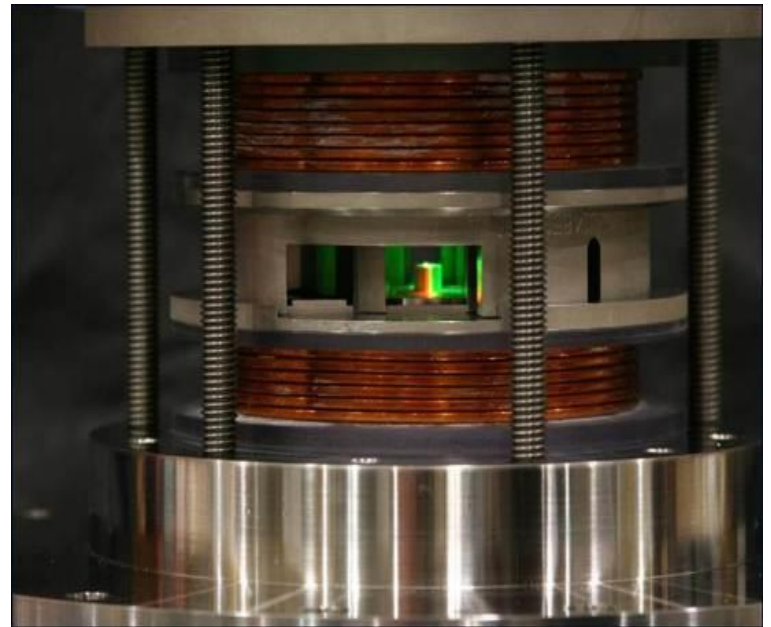
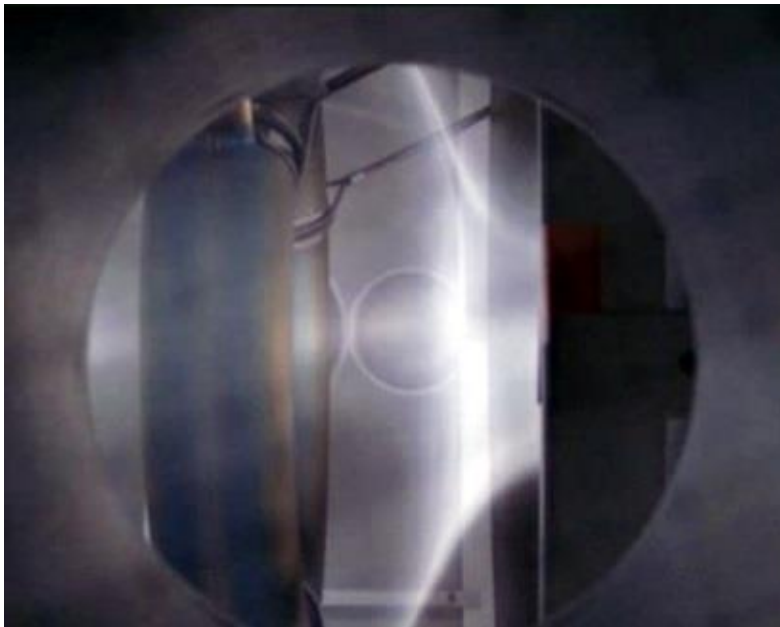
REFERENCES

1. S. Glasstone and R. H. Lovberg, "Controlled Thermonuclear Reactions, an Introduction to Theory and Experiment," Robert E. Krieger Publishing Company, Huntington, New York, 1975.
2. P. Caldirola and H. Knoepfel, "Physics of High Energy Density," Academic Press, New York and London, 1971.
3. M. Ragheb, "Gamma Rays Interactions with Matter," in: "Nuclear, Plasma and Radiation Science. Inventing the Future," <https://netfiles.uiuc.edu/mragheb/www>, 2011.
4. Robert W. Bussard, "The Advent of Clean Nuclear Fusion: Superperformance Space Power and Propulsion," 57th International Astronautical Congress, Valencia, Spain, October 2-6, 2006.
5. I. Langmuir and K. B. Blodgett, "Currents Limited by Space Charge between Concentric Spheres," Research laboratory, General Electric Company, Schenectady, New York, February 9, 1924.
6. Philo T. Farnsworth, "Electric Discharge Device for producing Interactions between Nuclei: USA patent no. 3,258,402, June 28, 1966.
7. R. L. Hirsch, "Inertial-Electrostatic Confinement of Ionized Fusion Gases," J. Appl. Phys., Vol. 38, No. 11, p. 4522, October 1967.
8. George H. Miley, Yibin Gu DeMora, J. M. Stubbers, R. A. Hochberg, T. A. Nadler, J. H. Anderi, "Discharge Characteristics of the Spherical Inertial Electrostatic Confinement (IEC) Device," Plasma Science, IEEE Transactions, pp. 733-739, August 1997.
9. Magdi Ragheb, George Miley, James Stubbins and Chan Choi, "Alternate Approach to Inertial Confinement Fusion with Low Tritium Inventories and High Power Densities, Journal of Fusion Energy, Vol. 4, Number 5, pp. 339-351, October 1985.
10. M. M. H. Ragheb, R. T. Santoro, J. M. Barnes, and M. J. Saltmarsh, "Nuclear Performance of Molten Salt Fusion-Fission Symbiotic Systems for Catalyzed Deuterium and Deuterium-Tritium Reactors," Nuclear Technology, Vol. 48, pp. 216-232, May 1980.
11. M. Ragheb, "Optimized Fissile and Fusile Breeding in a Laser-Fusion Fissile-Enrichment Flux Trap Blanket," Journal of Fusion Energy, Vol. 1, No.1, pp.285-298, 1981.
12. M. M. H. Ragheb, G. A. Moses, and C. W. Maynard, "Pellet and Pellet-Blanket neutronics and Photonics for Electron Beam Fusion," Nucl. Technol., Vol. 48:16, April 1980.
13. M. Ragheb and S. Behtash, "Symbiosis of Coupled Systems of Fusion D-3He Satellites and Tritium and He³ Generators," Nuclear Science and Engineering, Vol. 88, pp. 16-36, 1984.
14. M. Ragheb and C. W. Maynard, "On a Nonproliferation Aspect of the Presence of U²³² in the U²³³ fuel cycle," Atomkernenergie, 1979.
15. M. M. H. Ragheb, M. Z. Youssef, S. I. Abdel-Khalik, and C. W. Maynard, "Three-Dimensional Lattice Calculations for a Laser-Fusion Fissile Enrichment Fuel Factory," Trans. Am. Nucl. Soc., Vol. 30, 59, 1978.
16. M. M. H. Ragheb, S. I. Abdel-Khalik, M. Youssef, and C. W. Maynard, "Lattice Calculations and Three-Dimensional Effects in a Laser Fusion-Fission Reactor," Nucl. Technol. Vol. 45, 140, 1979.
17. H. A. Bethe, "The Fusion Hybrid," Nucl. News, Vol. 21, 7, 41, May 1978.
18. S. S. Rozhkov and G. E. Shatalov, "Thorium in the Blanket of a Hybrid Thermonuclear Reactor," Proc. U.S.-USSR Symp. Fusion-Fission Reactors, July 13-16, 1976, CONF-760733, p. 143, 1976.
19. V. L. Blinkin and V. M. Novikov, "Symbiotic System of a Fusion and Fission Reactor with Very Simple Fuel Reprocessing," Nucl. Fusion, Vol. 18, 7, 1978.
20. Jungmin Kang and Frank N. von Hippel, "U-232 and the Proliferation Resistance of U-233 in Spent Fuel," Science and Global Security, Volume 9, pp. 1-32, 2001.
21. J. A. Maniscalco, L. F. Hansen, and W. O. Allen, "Scoping Studies of U233 breeding fusion fission hybrid," UCRL-80585, Lawrence Livermore Laboratory, 1978.
22. L. M. Lidsky, "Fission-fusion Systems: Hybrid, Symbiotic and Augean," Nucl. Fusion, Vol. 15, 1975.
23. J. D. Lee, "The Beryllium/molten salt blanket-a new concept," UCRL-80585, Lawrence Livermore Laboratory, 1979.
24. M. M. H. Ragheb and C. W. Maynard, "Three-dimensional cell calculations for a fusion reactor gas-cooled solid blanket," Atomkernenergie (ATKE) Bd. 32, Lfg. 3, 159, 1978.
25. Monish Singh, "Fail-Safe Source-Driven Fission and Fusion-Fission Hybrid Reactors Configurations," M. Sc. Thesis, University of Illinois at Urbana-Champaign, 2012.

APPENDIX

Source: Lockheed-Martin

At the Google “Solve for X” conference on February 7, 2013, Lockheed Martin's long-term Advanced Development Programs department, known as “Skunk Works,” announced that Lockheed-Martin researchers are working on a high-beta, few open-field lines, good-curvature of the magnetic field lines, fourth generation compact DT or DD fusion reactor designated as T4. The development timeline introduces plans to have a prototype of a 100-MW nuclear fusion machine tested in 2017, and that a fully operational machine should be grid-ready by 2023.



T4 compact high-beta Tokamak. Source: Lockheed-Martin.

APPENDIX

Source: Lockheed-Martin

